Electronic Supplementary Information

Synthetic access to Calix[3]pyrroles via *meso*-Expansion: Hosts with diverse Guest Chemistry

B. Sathish Kumar, Narendra N. Pati, K. V. Jovan Jose and Pradeepta K. Panda*

School of Chemistry, University of Hyderabad, Hyderabad, India, 500046

Email: pkpsc@uohyd.ernet.in; pradeepta.panda@uohyd.ac.in

Contents:

1) Instrumentation and reagents **S2**
2) Synthesis **S3**
3) ^{1}H NMR & ^{13}C NMR spectra and HRMS data of compounds **S6**
4) X-ray crystal structure analysis **S14**
5) Photophysical study **S22**
6) Anion binding study **S23**
7) Computational study **S34**
8) References **S46**

1) Instrumentation and reagents:

Melting points were determined on MR-Vis+ visual melting point range apparatus from LABINDIA instruments private limited. IR spectra were recorded on Bruker FT-IR spectrometer. HRMS data were recorded with Bruker Maxis spectrometer. NMR spectra were recorded on a Bruker Avance-400 and 500 MHz FT NMR spectrometer using tetramethylsilane (TMS, $\delta = 0$) as an internal standard at room temperature. Crystallographic data for **5, 6** and **7** were collected on BRUKER APEX-II CCD microfocus diffractometer, Mo-K_α ($\lambda = 0.71073$ Å) radiation was used to collect X-ray reflections from the single crystal. Data reduction was performed using Bruker SAINT[1] software. Intensities for absorption were corrected by using SADABS 2014/5,[2] structure solution and refinement was done by using SHELXS-97,[3a] and SHELXL-2014/7[3b] with anisotropic displacement parameters for non-H atoms. Hydrogen atoms on O and N were experimentally located in difference electron density maps. All C−H atoms were fixed geometrically using HFIX command in SHELX-TL. A check of the final CIF file using PLATON[4] did not show any missed symmetry.

Crystallographic data (including the structure factor files) for structures **5, 6** and **7** in this paper have been deposited in the Cambridge Crystallographic Data Centre as supplementary publication number **CCDC 1954846, 1954847** and **1954848** respectively. Copies of the data can be obtained free of charge on application to CCDC, 12 Union Road, Cambridge CB2 1EZ, UK (Fax: +44(0)-1223-336033 or e-mail: deposit@ccdc.cam.ac.uk).

UV-vis spectra were recorded on Perkin Elmer Lambda 35 and Lambda 750 UV-VIS-NIR spectrophotometer. Fluorescence spectra were recorded on Horiba Fluorolog-FL3-221 spectrofluorometer. Fluorescence quantum yield was determined by use of comparative actinometry method and 9,10-diphenylanthracene (DPA) was used as the reference standard (Φ_{Δ}^{std} = 0.95 in ethanol).

All anions employed for anion binding studies are in the form of their tetrabutylammonium (TBA) salts (fluoride salt is in its trihydrate form). The receptor solutions were titrated by adding known quantities of concentrated solution of the anions in question. All tetrabutylammonium salts for NMR, UV-vis titrations were purchased from Sigma-Aldrich and were directly used in the titration experiment. The solvent used in the NMR and UV-vis titrations were purchased from Sigma-Aldrich and used as such.

The geometry optimization of the molecules is performed at MPW1PW91 density functional[5,6] and 6-31G(d,p)[7] basis function using the Gaussian 09 suite of packages.[8] The stationary points on the potential energy surface (PES) were characterized by the absence of imaginary harmonic vibrational modes. The UV-VIS absorption and emission spectra calculations were carried out on the optimized structures at BP86 density functional, with 6-311G(d) basis set[7] for the main group atoms. The solvation effect is incorporated using the implicit solvent model, solvation model based on density (SMD)[9], with acetonitrile as the solvent, as implemented in the Gaussian 09 packages.[8]

2) Synthesis:

2.1) Synthesis of compound 5:

Scheme S1:

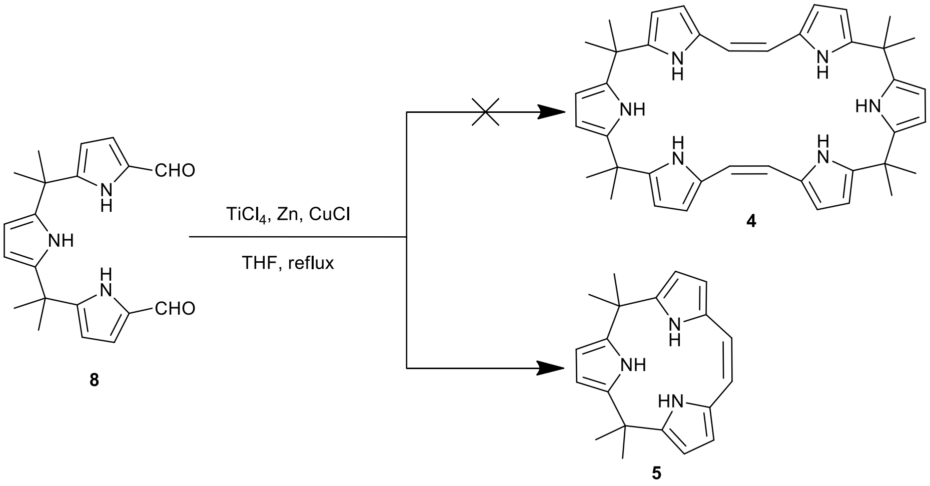

Dry THF (300 mL), Zn dust (3.88 g, 59.34 mmol) and CuCl (0.587 g, 5.93 mmol) were taken in a three neck round bottom flask under nitrogen atmosphere. To this $TiCl_4$ (~ 3.3 mL, 30.02 mmol) was added slowly through syringe at rt. The reaction mixture was refluxed for 4 h. Then solution of the compound **8**^{10a} (0.5 g, 1.48 mmol in 200 ml dry THF) was added slowly (dropwise) at the same temperature in about 90 min. The reaction mixture was continued to reflux for another 10 min., then cooled to 5-10 ^{o}C and hydrolyzed by slow addition of sat. aq. K_2CO_3 solution. Then the biphasic mixture was filtered through celite, and the organic layer was separated, which was washed with water and brine solution. The organic layer was passed through anhyd. Na_2SO_4 and concentrated in rotary evaporator under reduced pressure. The yellow-red colored crude solid product was purified by using silicagel column chromatography with 2-5% EtOAc in hexanes as the eluent. After evaporation of solvent, pure product **5** was obtained as light yellow solid (0.246 g, 54%).

Characterization data for 5: Melting point: 160-162 °C; FTIR Data (KBr) cm^{-1}: 3434, 2965, 1244, 1035, 771. ^{1}H NMR (400 MHz, $CDCl_3$) δ in ppm: 8.20 (s, 2H), 8.01 (s, 1H), 6.00 (s, 2H), 5.99 – 5.97 (m, 2H), 5.96 (d, *J* = 2.8 Hz, 2H), 5.91 (t, *J* = 3.0 Hz, 2H), 1.66 (s, 12H). ^{13}C NMR (101 MHz, $CDCl_3$) δ in ppm: 143.7, 141.5, 128.5, 116.0, 109.9, 105.0, 104.0, 36.4, 27.4. HR-MS (ESI) m/z calcd. for $[M-H]^-$ $C_{20}H_{22}N_3$: 304.1814, found: 304.1808. UV-vis (CH_3CN) λ_{max} (log ε): 350 nm (3.75).

2.2) Synthesis of compound 6:

Scheme S2:

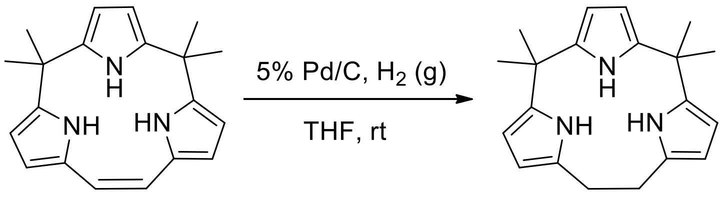

5 **6**

To the solution of compound **5** (0.165 g, 0.540 mmol) in dry THF (50 mL) containing triethylamine (2 µL, 0.014 mmol), 5% Pd/C (0.06 g, 0.028 mmol) was added. The reaction mixture was purged with H_2 gas and was stirred under H_2 atmosphere (using a balloon) for 18 h. Then the reaction mixture was filtered through celite and solvent was removed in rotary evaporator under reduced pressure. The crude solid product was purified by using silica gel column chromatography with 5% EtOAc in hexane as the eluent. Evaporation of the solvent resulted pure product **6** as white solid (103 mg, 62%).

Characterization data for 6: Melting point: 93-95 °C; FTIR Data (KBr) cm^{-1}: 3349, 2963, 1579, 1210, 1034, 766. ^{1}H NMR (400 MHz, $CDCl_3$) δ in ppm: 7.36 (s, 2H), 7.23 (s, 1H), 5.92 (t, *J* = 3.0 Hz, 2H), 5.86 (d, *J* = 2.8 Hz, 2H), 5.77 (t, *J* = 2.9 Hz, 2H), 2.75 (s, 4H), 1.59 (s, 12H). ^{13}C NMR (126 MHz, $CDCl_3$) δ in ppm: 139.4, 138.8, 131.5, 105.0, 104.0, 102.6, 36.1, 29.3, 27.5. HR-MS (ESI) m/z calcd. for $[M+H]^+$ $C_{20}H_{26}N_3$: 308.2127, found: 308.2120.

2.3) Synthesis of compound 7

Scheme S3:

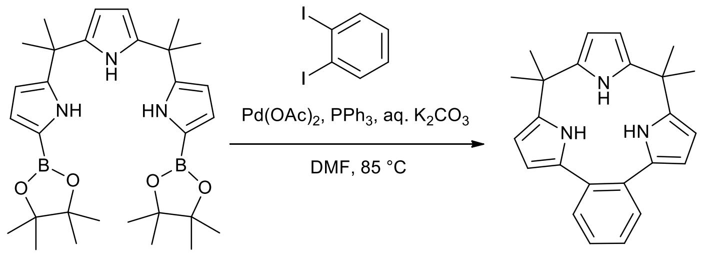

9 **7**

2,2’-Diboryl tripyrromethane **9** (1 g, 1.875 mmol), 1,2-diiodobenzene (0.240 mL, 1.837 mmol), $Pd(OAc)_2$ (0.084 g, 0.375 mmol), and PPh_3 (0.196 g, 0.75 mmol) were taken in a two neck round bottom flask which was evacuated and filled with N_2 gas. To this dry DMF (70 mL) was added and after stirring for 5 min. at rt, 2M aq. K_2CO_3 solution (18 mL) was added. Then the reaction mixture was stirred at 80-85 °C for 2 days. The reaction mixture was cooled and concentrated in rotary evaporator under vacuum. The crude solid was dissolved in DCM (20 mL) and washed with water (10 mL), then the organic layer was separated, washed with brine and concentrated in rotary evaporator under reduced pressure. Thus obtained crude solid was purified by silica gel column chromatography with 5% EtOAc in hexane as the eluent. Subsequent evaporation of the solvent yielded the pure product **7** as white solid (55 mg, 8%).

Characterization data for 7: Melting point: 199-201 °C; FTIR Data (KBr) cm^{-1}: 3432, 3371, 2959, 1260, 1034, 773. ^1H NMR (400 MHz, $CDCl_3$) δ in ppm: 7.60 (s, 2H), 7.41 (dd, *J* = 5.7, 3.4 Hz, 2H), 7.26 (dd, *J* = 5.7, 3.4 Hz, 2H), 7.17 (s, 1H), 6.06 (dt, *J* = 9.1, 3.2 Hz, 4H), 5.90 (d, *J* = 2.8 Hz, 2H), 1.64 (s, 12H). ^{13}C NMR (101 MHz, $CDCl_3$) δ in ppm: 141.3, 140.3, 132.7, 131.1, 130.7, 127.5, 108.0, 104.8, 103.4, 36.5, 28.0. HR-MS (ESI) m/z calcd. for $[M+H]^+$ $C_{20}H_{26}N_3$: 308.2127, found: 308.2120. UV-vis (CH_3CN) λ_{max} (log ε): 284 nm (4.11); Emission (CH_3CN) λ_{max} (λ_{ex} = 280 nm): 425 nm; Φ_Δ = 0.48 (ref: 9,10-diphenylanthracene).

2.4) Synthesis of compound 9

Scheme S4:

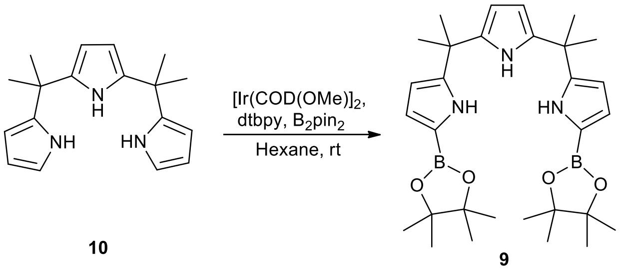

A two neck round bottom flask was dried in oven, which was cooled to rt under N_2 atmosphere. In this $[Ir(cod)(OMe)]_2$ (0.024 g, 0.036 mmol), 4,4′-di-tert-butyl-2,2′-dipyridyl (dtbpy) (0.019 g, 0.070 mmol) and bis(pinacolato)diboron (B_2pin_2) (0.894 g, 3.52 mmol) were added together and evacuated for 1 h, and filled with N_2 gas. To this dry hexane (20 mL) was added and stirred for few min. at rt, which resulted in a bright red color solution indicating the formation of the active catalyst. To this tripyrromethane **10**[10b] (0.66 g, 2.348 mmol) in dry hexane (50 mL) was added via syringe. The reaction mixture was stirred for another 15 h at rt. The solution of reaction mixture was washed with brine and the separated organic layer was passed through anhyd. Na_2SO_4 and concentrated in rotary evaporator under reduced pressure, resulted in a red colored solid **9** was pure enough (confirmed by ^1H NMR) to proceed for the next step (1 g, 80%).

Characterization data for 9: Melting point: 76-78 °C; FTIR Data (KBr) cm^{-1}: 3444, 2974, 1488, 1293, 1248, 1137, 1039, 777. ^1H NMR (400 MHz, $CDCl_3$) δ in ppm: 8.35 (s, 2H), 7.43 (s, 1H), 6.72 (dd, *J* = 3.5, 2.5 Hz, 2H), 6.01 (dd, *J* = 3.5, 2.6 Hz, 2H), 5.94 (d, *J* = 2.8 Hz, 2H), 1.59 (s, 12H), 1.29 (s, 25H). ^{13}C NMR (126 MHz, $CDCl_3$) δ in ppm: 144.5, 138.1, 120.6, 106.1, 103.7, 83.6, 35.8, 29.6, 24.9, 24.7. HR-MS (ESI) m/z calcd. for $[M+H]^+$ $C_{30}H_{46}B_2N_3O_4$: 534.3674, found: 534.3671.

3) ^{1}H NMR & ^{13}C NMR spectra and HRMS data of compounds:

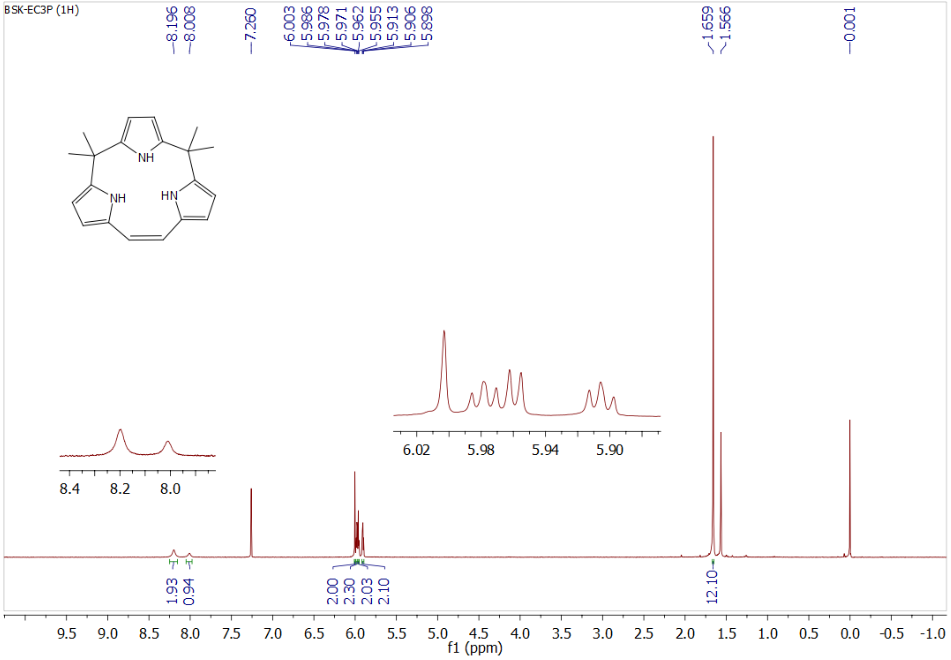

Figure S1: ^{1}H NMR spectrum of compound **5** in $CDCl_3$.

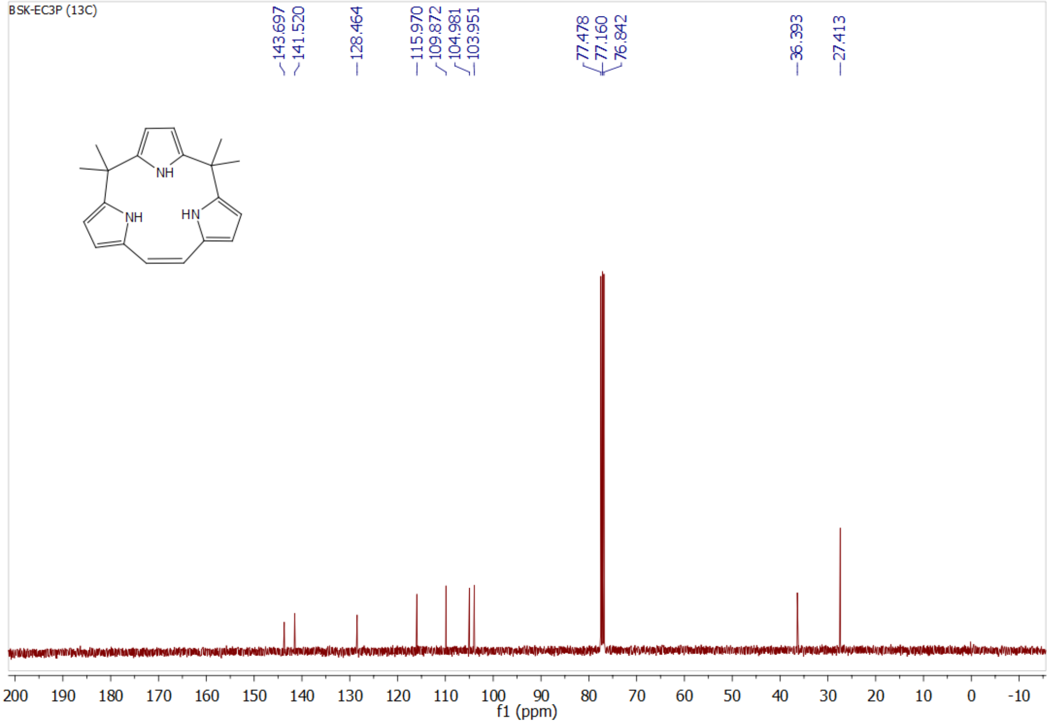

Figure S2: ^{13}C NMR spectrum of compound **5** in $CDCl_3$.

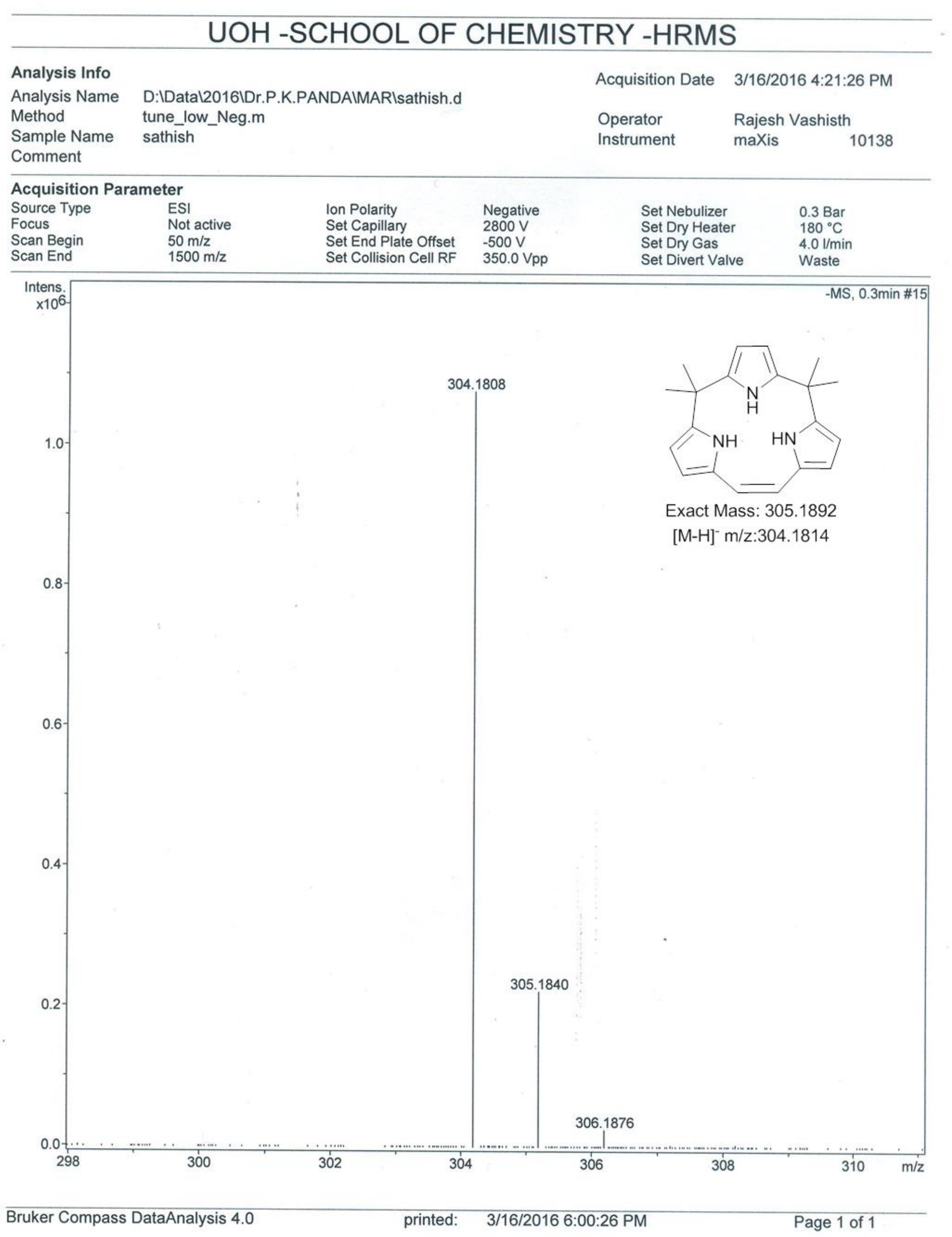

UOH -SCHOOL OF CHEMISTRY -HRMS

Analysis Info

Analysis Name	D:\Data\2016\Dr.P.K.PANDA\MAR\sathish.d	Acquisition Date	3/16/2016 4:21:26 PM
Method	tune_low_Neg.m	Operator	Rajesh Vashisth
Sample Name	sathish	Instrument	maXis 10138
Comment			

Acquisition Parameter

Source Type	ESI	Ion Polarity	Negative	Set Nebulizer	0.3 Bar
Focus	Not active	Set Capillary	2800 V	Set Dry Heater	180 °C
Scan Begin	50 m/z	Set End Plate Offset	-500 V	Set Dry Gas	4.0 l/min
Scan End	1500 m/z	Set Collision Cell RF	350.0 Vpp	Set Divert Valve	Waste

Bruker Compass DataAnalysis 4.0 printed: 3/16/2016 6:00:26 PM Page 1 of 1

Figure S3: HRMS data of compound **5**.

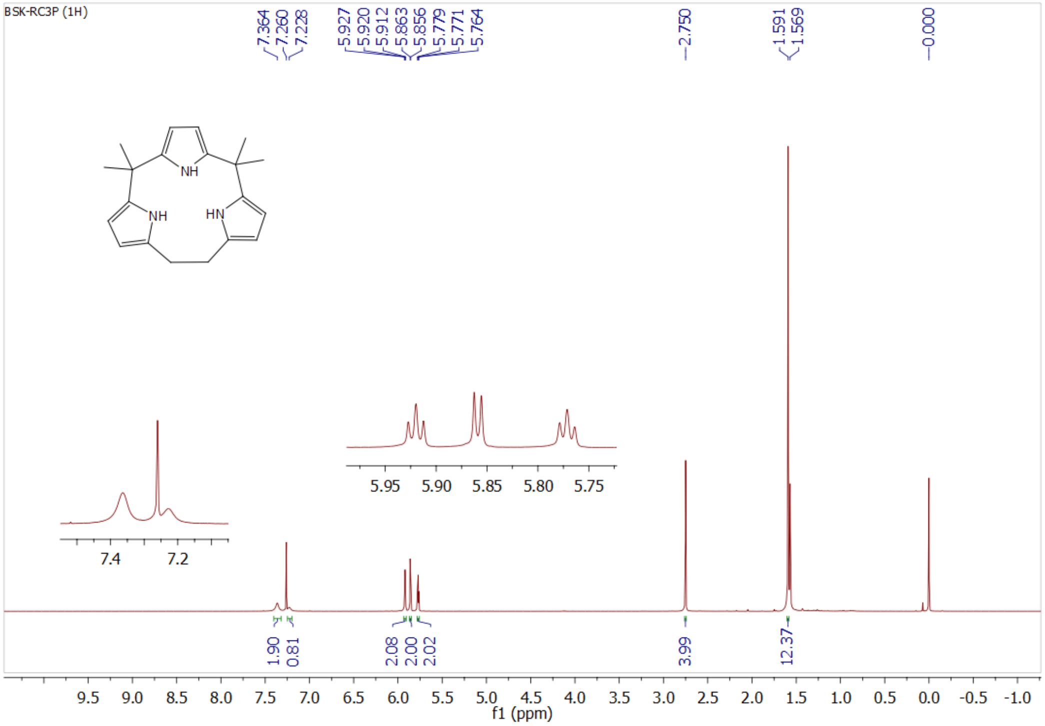

Figure S4: ^{1}H NMR spectrum of compound **6** in $CDCl_3$.

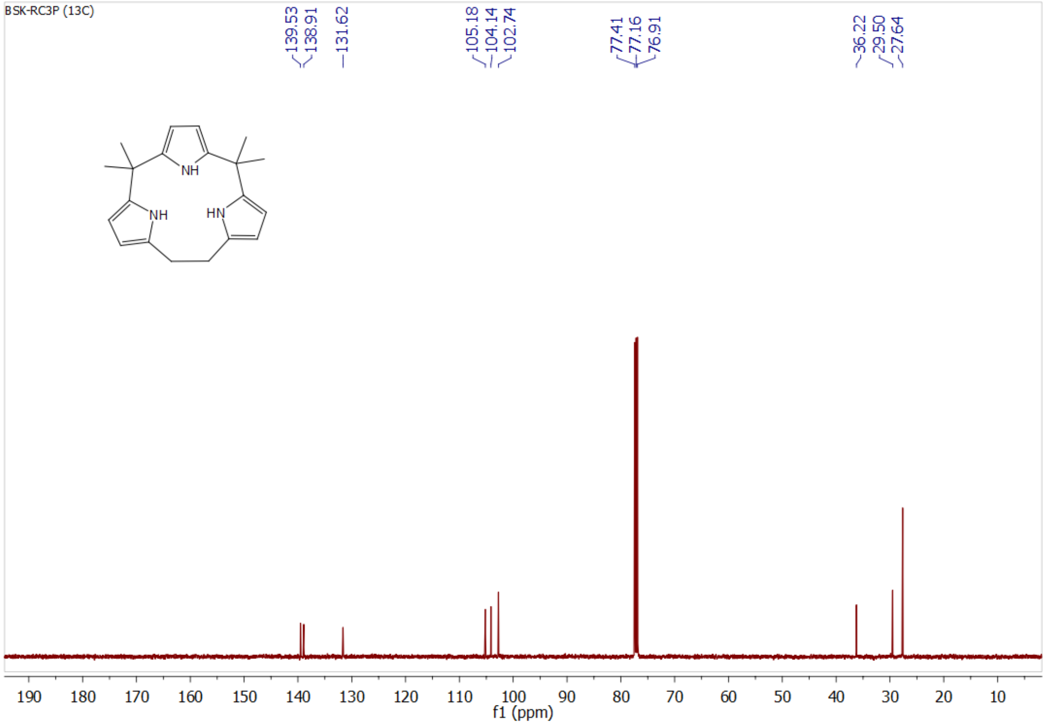

Figure S5: ^{13}C NMR spectrum of compound **6** in $CDCl_3$.

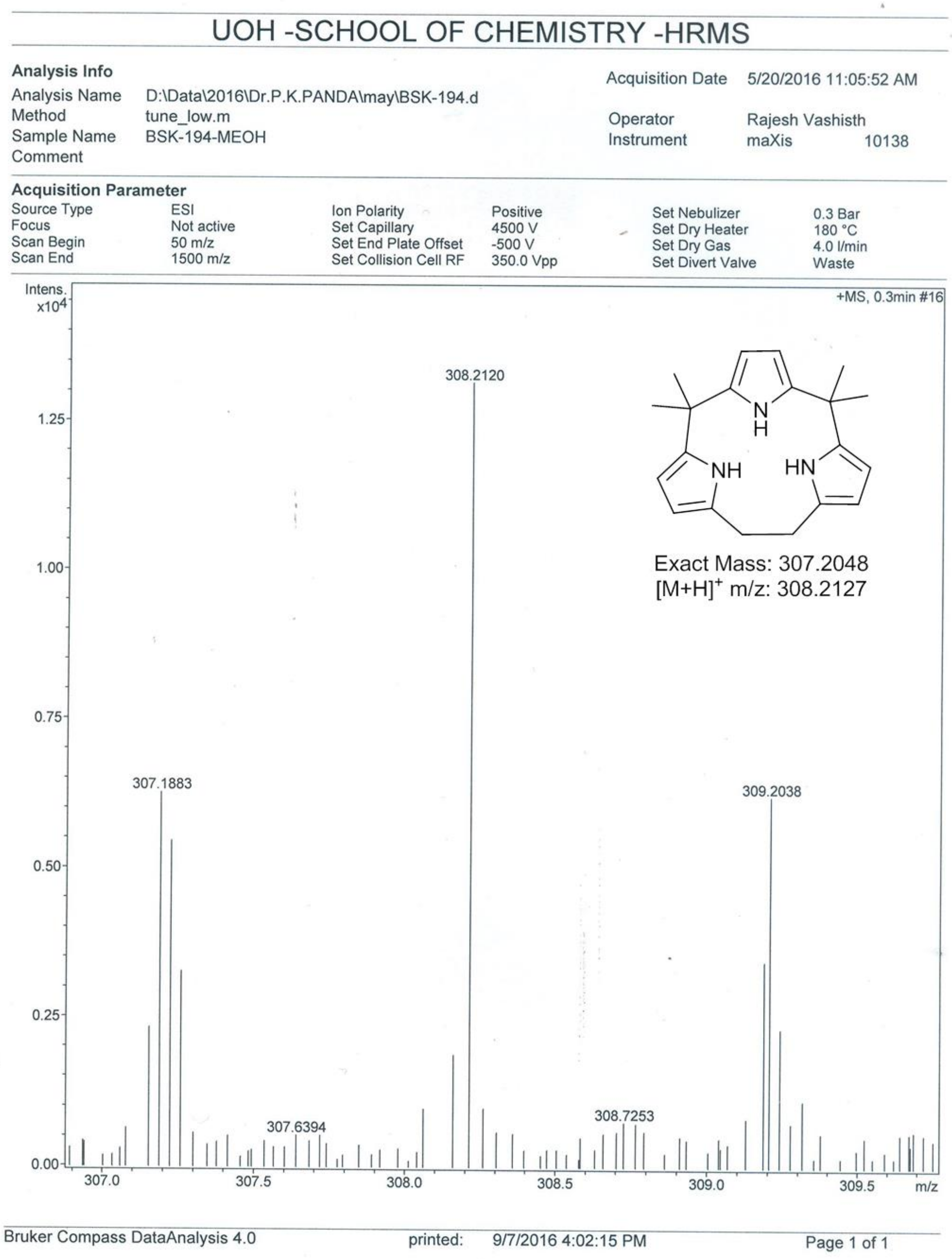

UOH -SCHOOL OF CHEMISTRY -HRMS

Analysis Info

Analysis Name D:\Data\2016\Dr.P.K.PANDA\may\BSK-194.d
Method tune_low.m
Sample Name BSK-194-MEOH
Comment

Acquisition Date 5/20/2016 11:05:52 AM

Operator Rajesh Vashisth
Instrument maXis 10138

Acquisition Parameter

Source Type	ESI	Ion Polarity	Positive	Set Nebulizer	0.3 Bar
Focus	Not active	Set Capillary	4500 V	Set Dry Heater	180 °C
Scan Begin	50 m/z	Set End Plate Offset	-500 V	Set Dry Gas	4.0 l/min
Scan End	1500 m/z	Set Collision Cell RF	350.0 Vpp	Set Divert Valve	Waste

Exact Mass: 307.2048
$[M+H]^+$ m/z: 308.2127

Bruker Compass DataAnalysis 4.0 printed: 9/7/2016 4:02:15 PM Page 1 of 1

Figure S6: HRMS data of compound **6**.

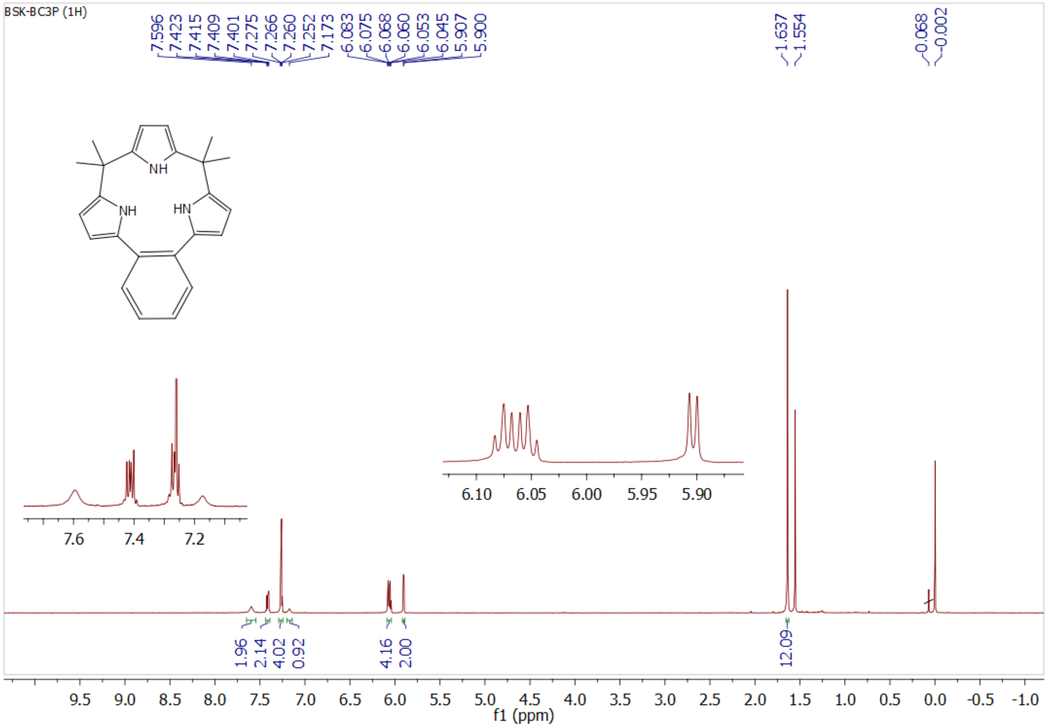

Figure S7: ^{1}H NMR spectrum of compound **7** in $CDCl_3$.

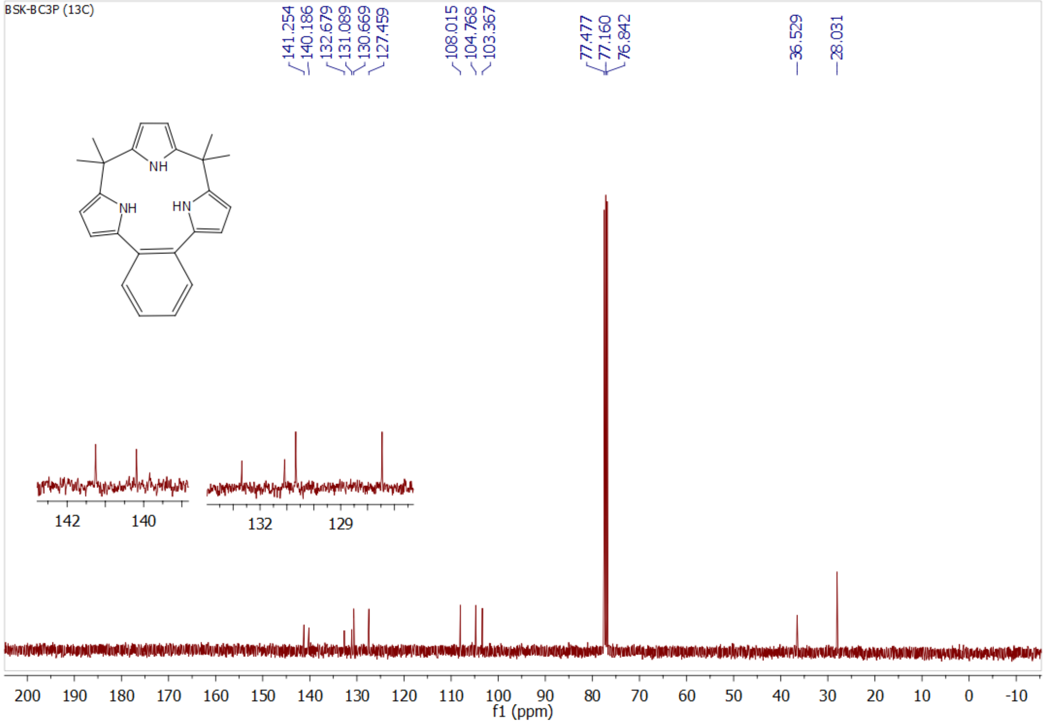

Figure S8: ^{13}C NMR spectrum of compound **7** in $CDCl_3$.

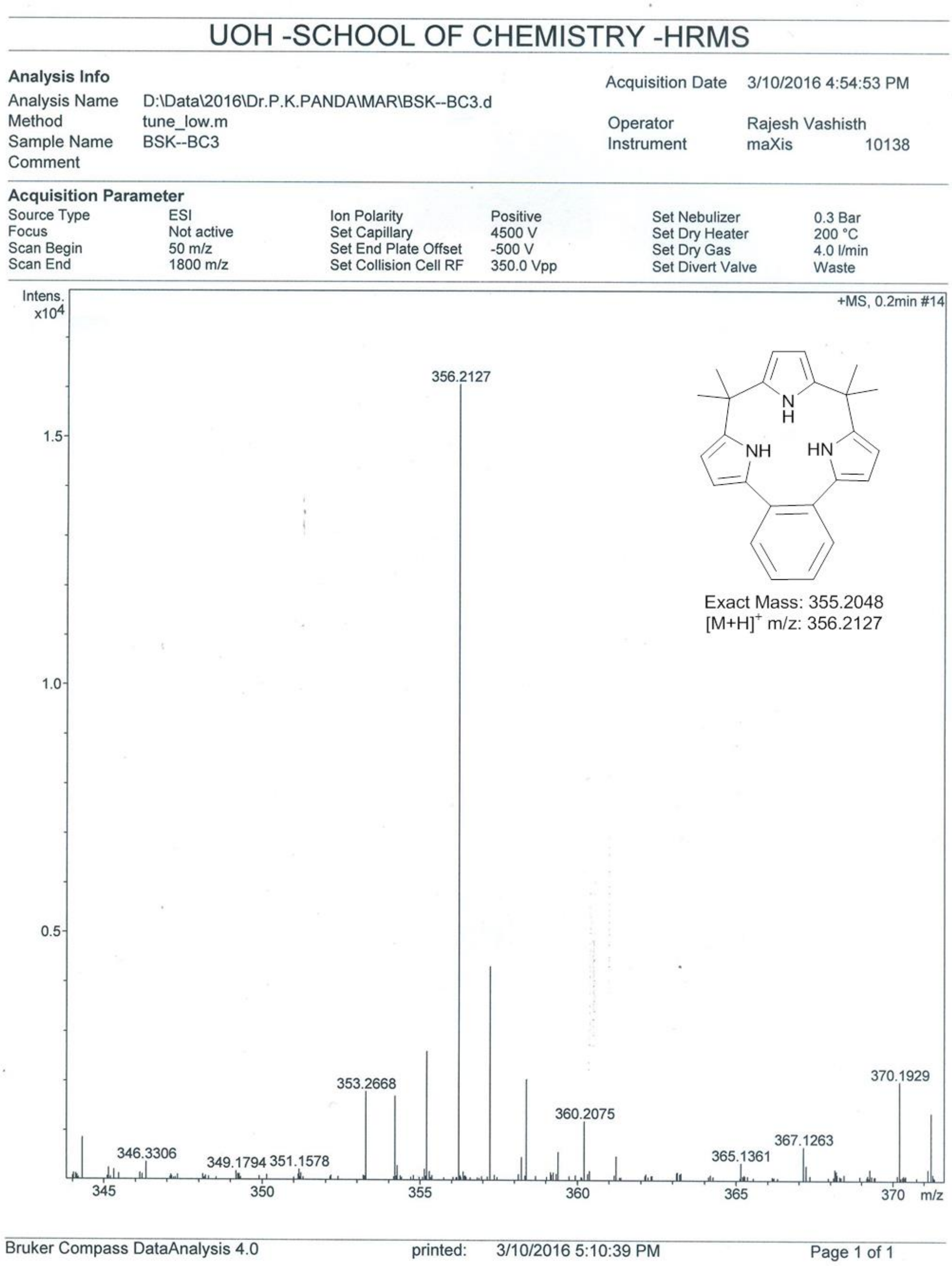

UOH -SCHOOL OF CHEMISTRY -HRMS

Analysis Info

Analysis Name	D:\Data\2016\Dr.P.K.PANDA\MAR\BSK--BC3.d	Acquisition Date	3/10/2016 4:54:53 PM
Method	tune_low.m	Operator	Rajesh Vashisth
Sample Name	BSK--BC3	Instrument	maXis 10138
Comment			

Acquisition Parameter

Source Type	ESI	Ion Polarity	Positive	Set Nebulizer	0.3 Bar
Focus	Not active	Set Capillary	4500 V	Set Dry Heater	200 °C
Scan Begin	50 m/z	Set End Plate Offset	-500 V	Set Dry Gas	4.0 l/min
Scan End	1800 m/z	Set Collision Cell RF	350.0 Vpp	Set Divert Valve	Waste

Exact Mass: 355.2048
$[M+H]^+$ m/z: 356.2127

Bruker Compass DataAnalysis 4.0 printed: 3/10/2016 5:10:39 PM Page 1 of 1

Figure S9: HRMS data of compound **7**.

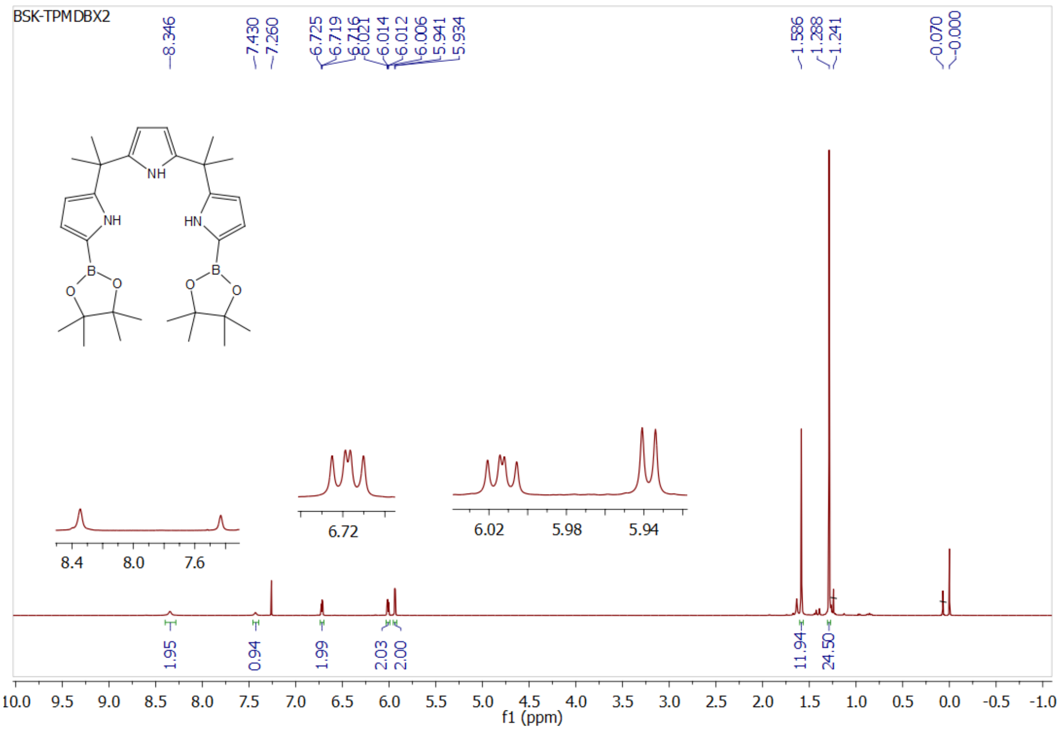

Figure S10: ^{1}H NMR spectrum of compound **9** in CDCl$_3$.

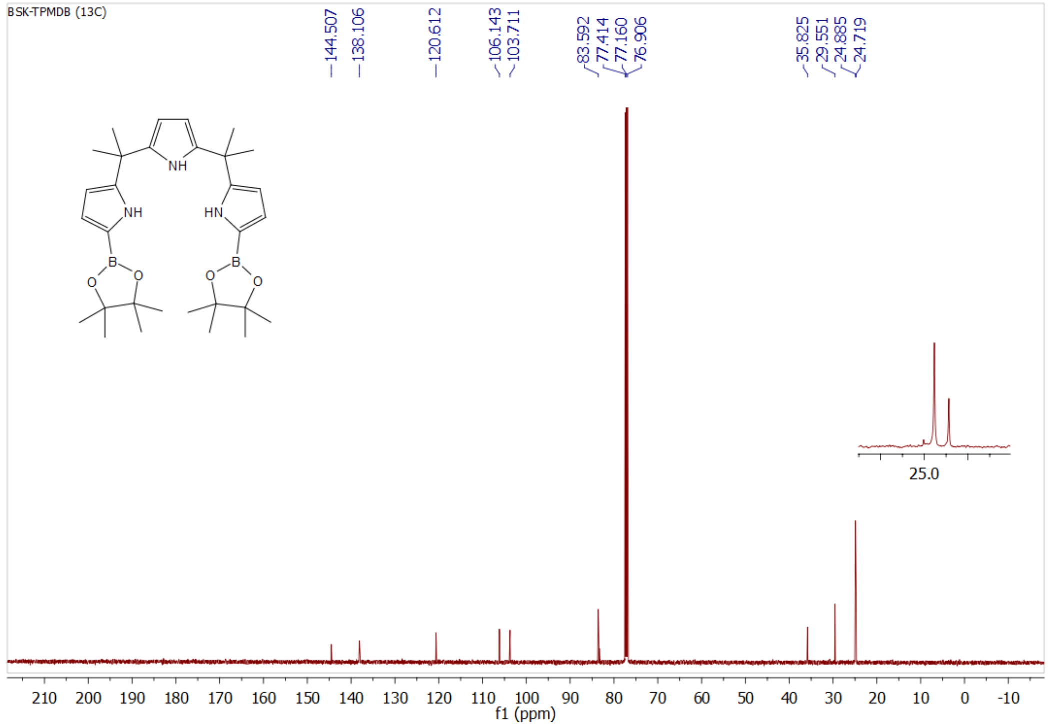

Figure S11: ^{13}C NMR spectrum of compound **9** in CDCl$_3$.

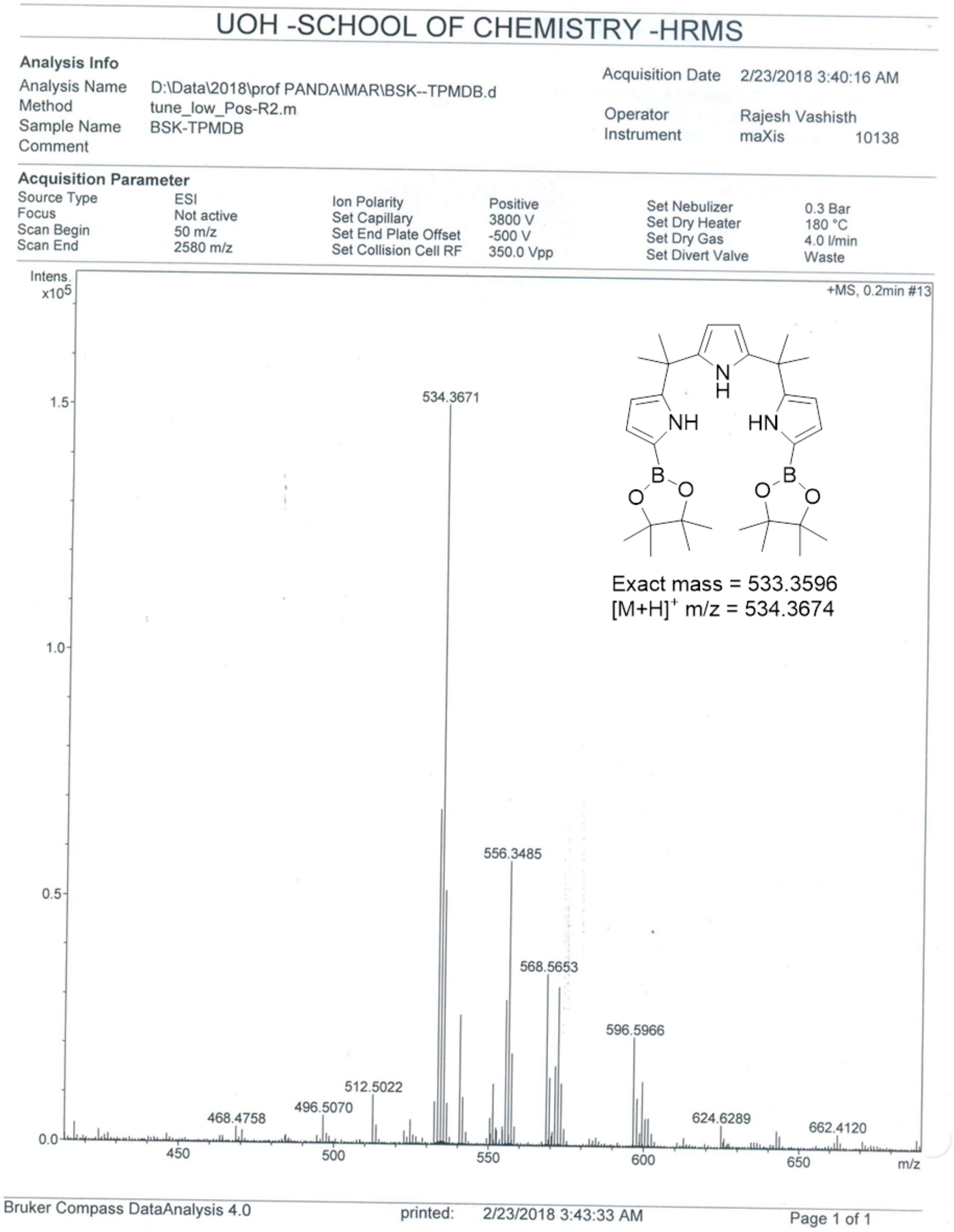

UOH -SCHOOL OF CHEMISTRY -HRMS

Analysis Info

Analysis Name D:\Data\2018\prof PANDA\MAR\BSK--TPMDB.d
Method tune_low_Pos-R2.m
Sample Name BSK-TPMDB
Comment

Acquisition Date 2/23/2018 3:40:16 AM
Operator Rajesh Vashisth
Instrument maXis 10138

Acquisition Parameter

Source Type ESI
Focus Not active
Scan Begin 50 m/z
Scan End 2580 m/z
Ion Polarity Positive
Set Capillary 3800 V
Set End Plate Offset -500 V
Set Collision Cell RF 350.0 Vpp
Set Nebulizer 0.3 Bar
Set Dry Heater 180 °C
Set Dry Gas 4.0 l/min
Set Divert Valve Waste

Exact mass = 533.3596
[M+H]$^+$ m/z = 534.3674

Bruker Compass DataAnalysis 4.0 printed: 2/23/2018 3:43:33 AM Page 1 of 1

Figure S12: HRMS data of compound **9**.

4) X-ray Crystal structure analysis:

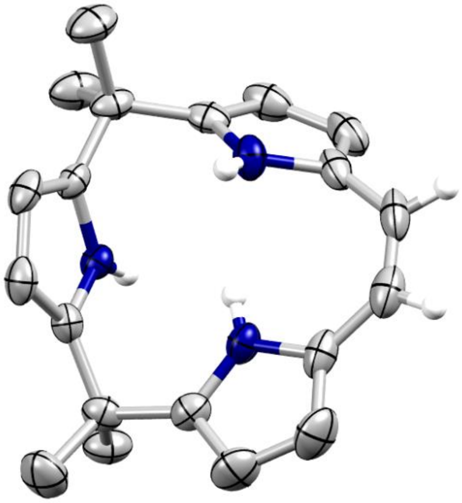

Figure S13: ORTEP-POVray diagram of macrocycle **5**; All hydrogens bound to methyl, *β*-pyrrolic carbon atoms are excluded for clarity; Thermal ellipsoids are scaled up to 35% probability level; Color code: grey = Carbon, white = Hydrogen and blue = Nitrogen.

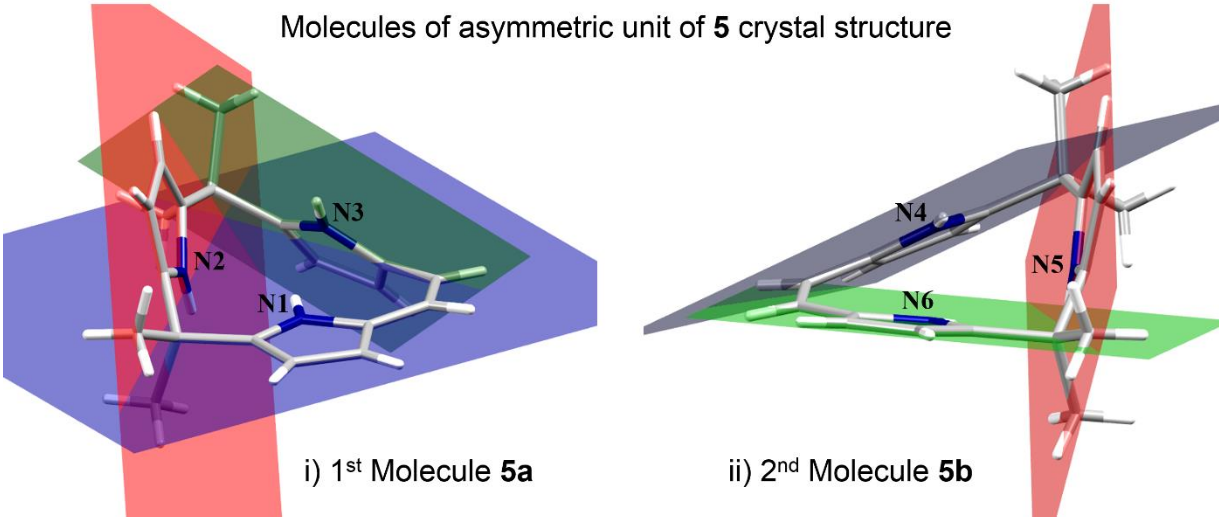

Molecules of asymmetric unit of **5** crystal structure

i) 1st Molecule **5a**

ii) 2nd Molecule **5b**

Figure S14: Capped stick view of the asymmetric unit of **5** represented with different planes passing through pyrrole units.

Table S1: Summary of angles between the planes and distances between nitrogen atoms of each molecule in the asymmetric unit of **5**.

Angle between planes			
	5a		**5b**
∠ Violet-Red	~ 101° (N1 vs N2)	∠ Grey-Red	~ 59° (N4 vs N5)
∠ Red-Green	~ 62° (N2 vs N3)	∠ Red-Green	~ 85° (N5 vs N6)
∠ Violet -Green	~ 50° (N1 vs N3)	∠ Grey-Green	~ 29° (N4 vs N6)

Distances	
5a	**5b**
2.909(3) Å (N1-N2)	2.893(3) Å (N4-N5)
2.988(3) Å (N2-N3)	2.938(3) Å (N5-N6)
2.954(4) Å (N1-N3)	2.885(3) Å (N4-N6)

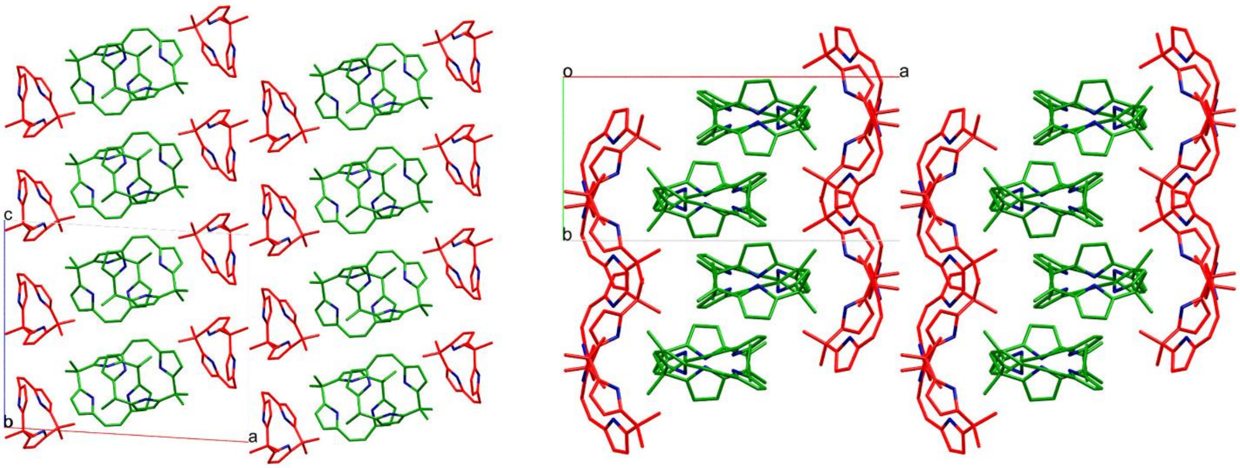
a) view along with b-axis

b) view along with c-axis

Figure S15: Packing diagram of **5** in capped-stick view. Color code: red **= 5a** and green = **5b**; hydrogen atoms are excluded for clarity.

Table S2: Crystal structure data with refinement information for **5**

Crystal data	**5**	
Formula	$C_{20}H_{23}N_3$	
Formula weight	305.41	
Color	Colorless	
Temperature	297(2) K	
Wavelength	0.71073 Å	
Crystal system	Monoclinic	
Space group	$P\ 2_1/c$	
Unit cell dimensions	a = 20.236(3) Å b = 9.7971(16) Å c = 17.139(3) Å Volume = 3391.6(9) $Å^3$	α = 90° β = 93.473(5)° ν = 90°
Z	8	
Density (calculated)	1.196 g/cm^3	
Absorption coefficient	0.072 mm^{-1}	
F(000)	608	
Crystal size	0.16 x 0.12 x 0.08 mm^3	
Theta range for data collection	2.310 to 25.716°	
Index ranges	-24<=h<=24, -11<=k<=11, -20<=l<=20	
Reflections collected	43978	
Independent reflections	6418 [R(int) = 0.1080]	
Completeness to theta	99.7 % (θ 25.242°)	
Absorption correction type	Multi-scan	
Max. and min. transmission	0.7453 and 0.6612	
Refinement method	Full-matrix least-squares on F^2	
Data / restraints / parameters	6418 / 0 / 448	
Goodness-of-fit on F^2	1.045	
Final R indices [I>2sigma(I)]	R1 = 0.0596, wR2 = 0.1575	
R indices (all data)	R1 = 0.1112, wR2 = 0.1849	
Extinction coefficient	n/a	
Largest diff. peak and hole	0.186 and -0.173 e.$Å^{-3}$	

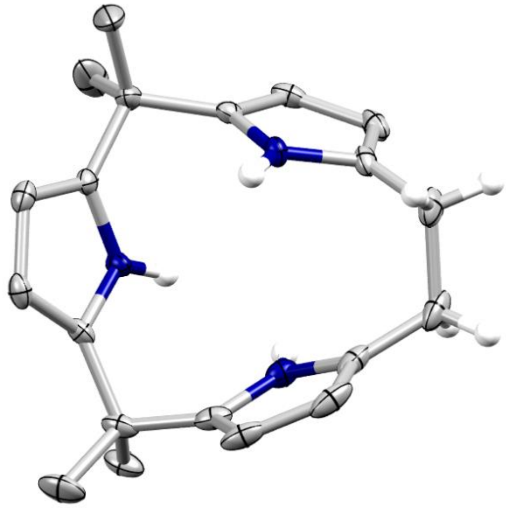

Figure S16: ORTEP-POVray diagram of macrocycle **6**; Solvent molecule (H_2O), all hydrogens bound to methyl, *β*-pyrrolic carbon atoms are excluded for clarity; Thermal ellipsoids are scaled up to 35% probability level; Color code: grey = Carbon, white = Hydrogen and blue = Nitrogen.

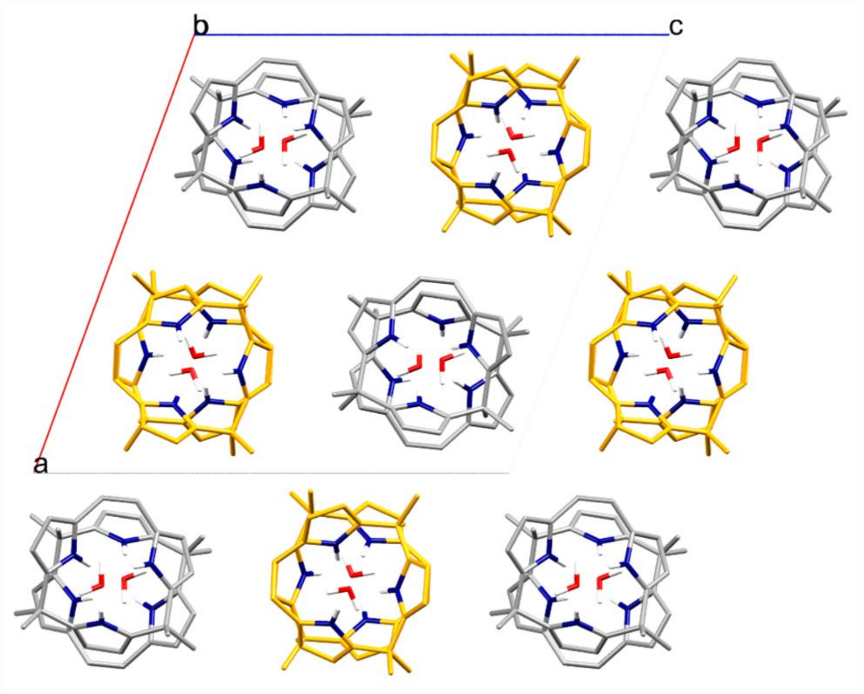

Figure S17: Packing diagram of **6** with two set of molecules shown in two different colors (as in asymmetric unit) in capped-stick view along with b-axis. All hydrogens bound to carbon atoms are excluded for clarity. Color code: grey and yellow = Carbon, white = Hydrogen, blue = Nitrogen and red = Oxygen.

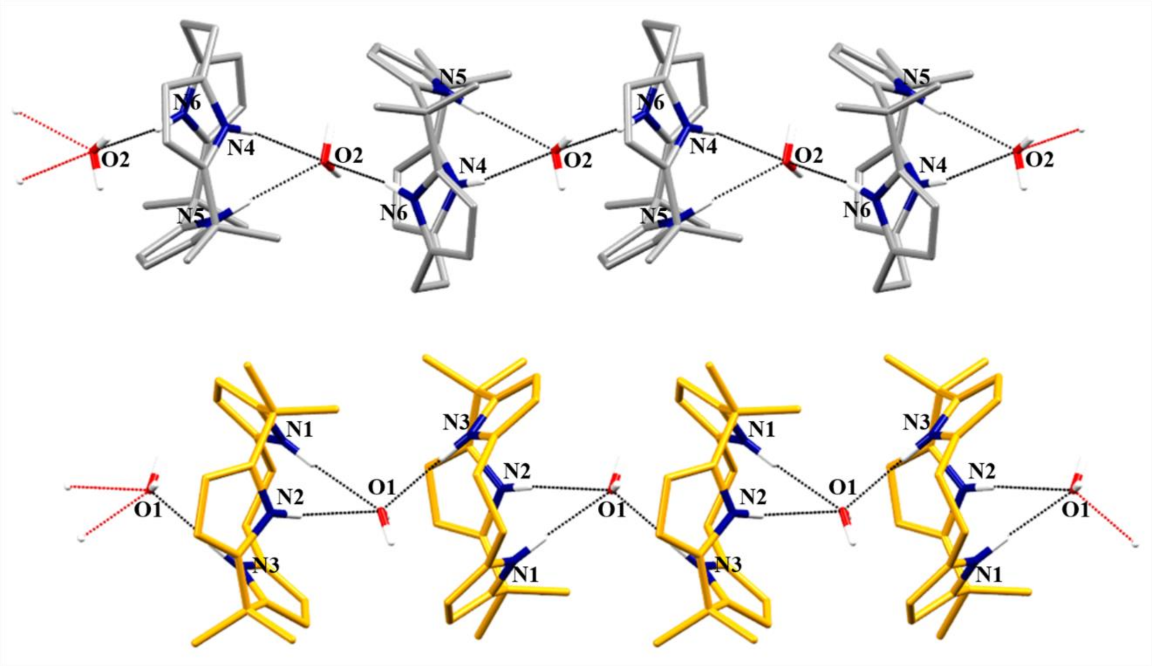

Figure S18: Packing diagram of **6** with two set of molecules (as in the asymmetric unit) in capped-stick view. All hydrogens bound to carbon atoms are excluded for clarity. Color code: grey and yellow = Carbon, white = Hydrogen, blue = Nitrogen and red = Oxygen. Hydrogen bonds are represented with black dashed lines and corresponding hanging contacts are in red dashed lines.

Table S3. Summary of hydrogen-bonding interactions of **6**.

D−H···A	**d(D−H)** (Å)	**d(H···A)** (Å)	**d(D···A)** (Å)	∠ **(D−H···A)** (°)
N1−H···O1	0.92(2)	2.13(2)	3.042(2)	173(2)
N2−H···O1	0.90(2)	2.42(2)	3.315(2)	170(2)
N3−H···O1	0.92(2)	2.10(2)	3.021(2)	178(2)
N4−H···O2	0.89(2)	2.36(2)	3.228(2)	166(2)
N5−H···O2	0.90(2)	2.17(2)	3.063(1)	176(2)
N6−H···O2	0.93(2)	2.20(2)	3.123(1)	171(2)

Table S4: Crystal structure data with refinement information for **$6\cdot H_2O$**

Crystal data	**$6\cdot H_2O$**
Formula	$C_{20} H_{27} N_3 O$
Formula weight	325.44
Color	Colorless
Temperature	123(2) K
Wavelength	0.71073 Å
Crystal system	Monoclinic
Space group	$P\ 2_1/n$
Unit cell dimensions	a = 18.2435(15) Å b = 11.4952(9) Å c = 18.5875(12) Å α = 90° β = 110.086(2)° ν = 90° Volume = 3660.9(5) Å^3
Z	8
Density (calculated)	1.181 g/cm^3
Absorption coefficient	0.074 mm^{-1}
F(000)	1408
Crystal size	0.14 x 0.08 x 0.06 mm^3
Theta range for data collection	2.227 to 25.737°
Index ranges	-22<=h<=22, -14<=k<=13, -21<=l<=22
Reflections collected	74905
Independent reflections	6968 [R(int) = 0.0519]
Completeness to theta	99.7 % (θ 25.242°)
Absorption correction type	Multi-scan
Max. and min. transmission	0.7453 and 0.6805
Refinement method	Full-matrix least-squares on F^2
Data / restraints / parameters	6968 / 0 / 481
Goodness-of-fit on F^2	1.070
Final R indices [I>2sigma(I)]	R1 = 0.0408, wR2 = 0.1304
R indices (all data)	R1 = 0.0503, wR2 = 0.1390
Extinction coefficient	n/a
Largest diff. peak and hole	0.255 and -0.212 e.Å^{-3}

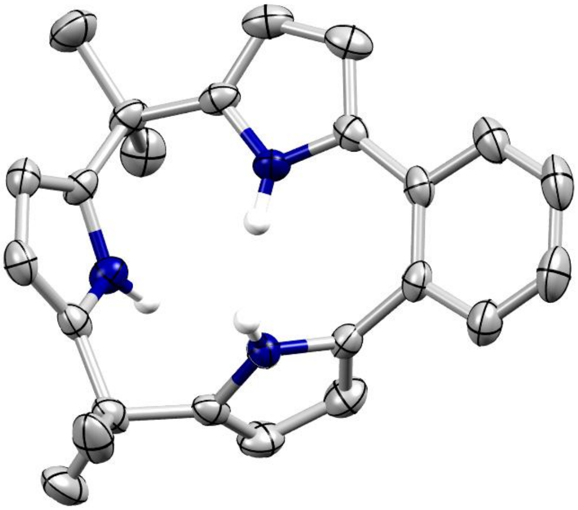

Figure S19: ORTEP-POVray diagram of macrocycle **7**; All hydrogens bound to methyl, β-pyrrolic and benzene carbon atoms are excluded for clarity; Thermal ellipsoids are scaled up to 35% probability level; Color code: grey = Carbon, white = Hydrogen and blue = Nitrogen.

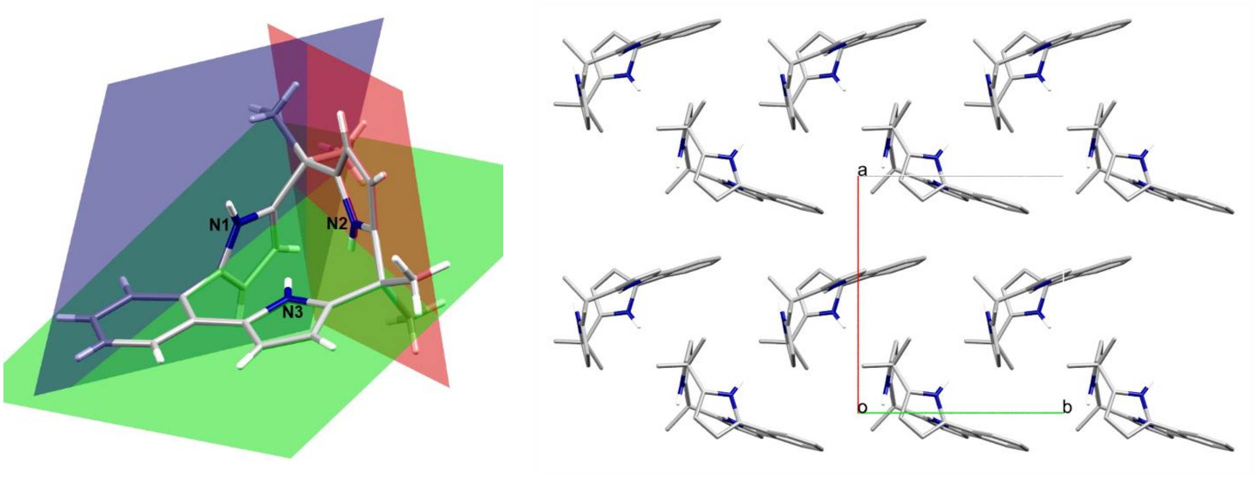

a) representation via different planes

b) packing diagram

Figure S20: Capped stick view of **7** represented with different planes passing through pyrrole units **(a)** and corresponding packing diagram view along with c-axis **(b)**.

Table S5: Summary of angles between the planes of **7** and intramolecular nitrogen atom distances.

(N1 - N2)		**(N2 - N3)**		**(N1 - N3)**	
∠ Violet-Red	distance	∠ Red-Green	distance	∠ Violet-Green	distance
67.22°	3.120(3) Å	78.30°	2.936(3) Å	76.83°	3.097(3) Å

Table S6: Crystal structure data with refinement information for **7**

Crystal data	**7**
Formula	$C_{24}\ H_{25}\ N_{3}$
Formula weight	355.47
Color	Colorless
Temperature	299(2) K
Wavelength	0.71073 Å
Crystal system	Monoclinic
Space group	$P\ 2_1/n$
Unit cell dimensions	a = 11.3125(17) Å | α = 90° b = 9.7429(13) Å | β = 95.103(5)° c = 17.745(3) Å | ν = 90° Volume = 1948.1(5) $Å^3$
Z	4
Density (calculated)	1.212 g/cm^3
Absorption coefficient	0.072 mm^{-1}
F(000)	760
Crystal size	0.28 x 0.24 x 0.18 mm^3
Theta range for data collection	2.228 to 25.119°
Index ranges	-13<=h<=13, -11<=k<=11, -21<=l<=21
Reflections collected	47223
Independent reflections	3477 [R(int) = 0.1477]
Completeness to theta	99.9 % (θ 25.119°)
Absorption correction type	Multi-scan
Max. and min. transmission	0.7452 and 0.6825
Refinement method	Full-matrix least-squares on F^2
Data / restraints / parameters	3477 / 0 / 261
Goodness-of-fit on F^2	1.036
Final R indices [I>2sigma(I)]	R1 = 0.0603, wR2 = 0.1496
R indices (all data)	R1 = 0.1080, wR2 = 0.1727
Extinction coefficient	0.013(2)
Largest diff. peak and hole	0.222d -0.146 e.$Å^{-3}$

5) Photophysical study:

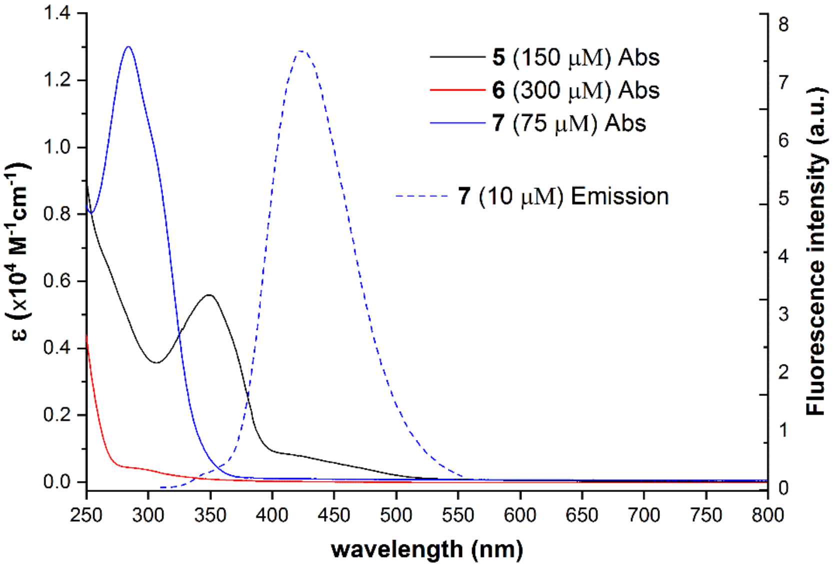

Figure S21: Absorption and emission spectra of calix[3]pyrroles (**5-7**) in acetonitrile.

Table S7: Photophysical data of calix[3]pyrroles (**5-7**) and expanded analogues (**3a and 3b**) in acetonitrile.

	5	**6**	**7**	**3a** [11a]	**3b** [11b]
Abs (λ_{max}) (nm)	350	293	284	316	284, 303
log ε	3.75	2.61	4.11	4.40	4.88
Emission (λ_{max}) (nm)	-	-	425 (λ_{ex} = 280 nm)	-	420 (λ_{ex} = 292 nm)

6) Anion binding study:

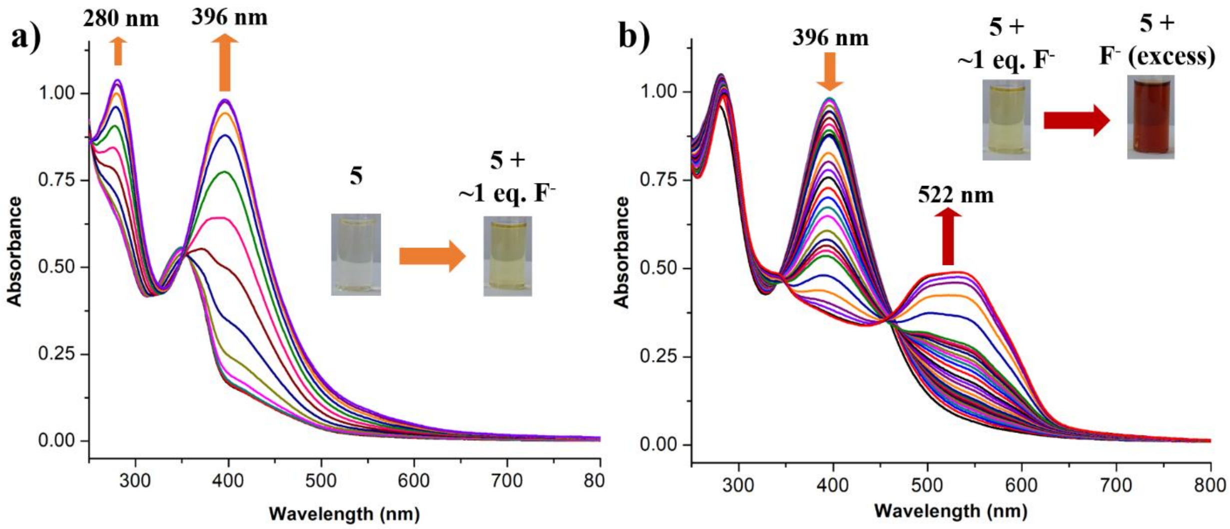

Figure S22: UV-vis spectral changes and corresponding colorimetric response of **5** (120 µM) after gradual addition of TBAF·3H$_2$O [a) 0 - 1eq. F$^-$ b) 1-50 eq. F$^-$] in acetonitrile.

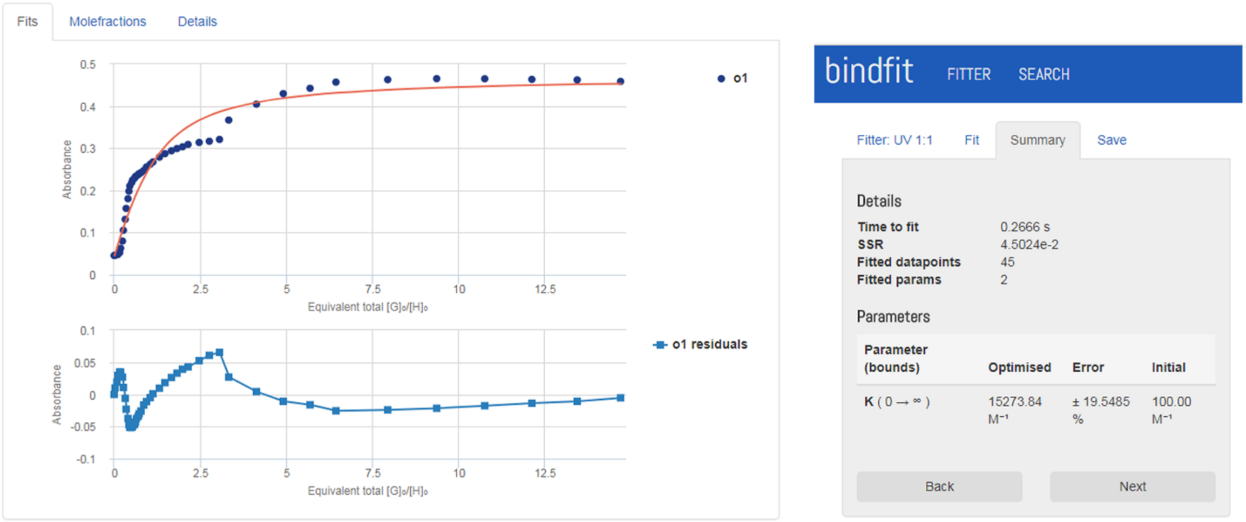

Details

Time to fit 0.2666 s
SSR 4.5024e-2
Fitted datapoints 45
Fitted params 2

Parameters

Parameter (bounds)	Optimised	Error	Initial
K (0 → ∞)	15273.84 M^{-1}	± 19.5485 %	100.00 M^{-1}

Figure S23: Assessment of binding constant (K_a) by UV-vis titration study of **5** (120 µM) with the gradual addition of TBAF·3H$_2$O in acetonitrile, the absorbance at 490 nm was plotted against fluoride concentration.[12]

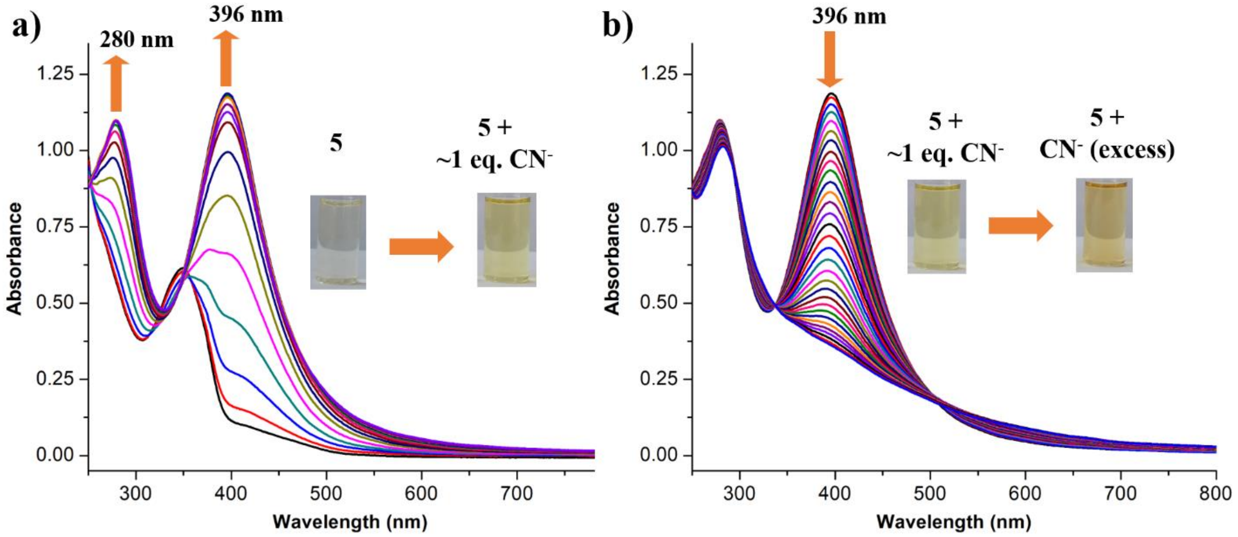

Figure S24: UV-vis spectral changes and corresponding colorimetric response of **5** (120 µM) after the gradual addition of TBACN [a) 0 - 1eq. CN^- b) 1-50 eq. CN^-] in acetonitrile.

Details

Time to fit	2.7275 s
SSR	0.3419
Fitted datapoints	46
Fitted params	4

Parameters

Parameter (bounds)	Optimised	Error	Initial
K_{11} (0 → ∞)	519836.52 M^{-1}	± 43.8825 %	1000.00 M^{-1}
K_{21} (0 → ∞)	38253.33 M^{-1}	± 19.0664 %	100.00 M^{-1}

Figure S25: Assessment of binding constant (K_a) by UV-vis titration study of **5** (120 µM) with gradual addition of TBACN in acetonitrile, the absorbance at 396 nm was plotted against cyanide concentration.[13]

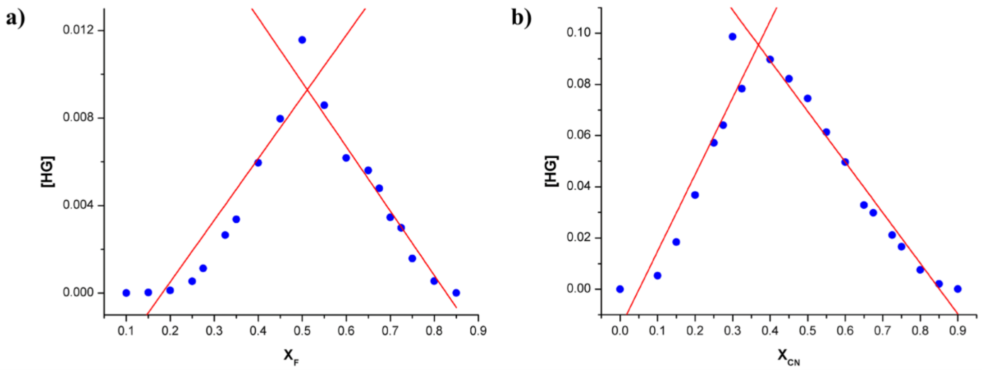

Figure S26: Job's plot analysis performed by UV-vis spectral changes for **5** (120 µM) in acetonitrile; (a) **5** vs TBAF·3H_2O and (b) **5** vs TBACN.

Limit of detection (LOD) calculation:[14]

LOD = 3.3 x σ / S

where σ = the standard deviation of the response

(the standard deviation of the y-intercept of regression lines)

S = the slope of the calibration curve

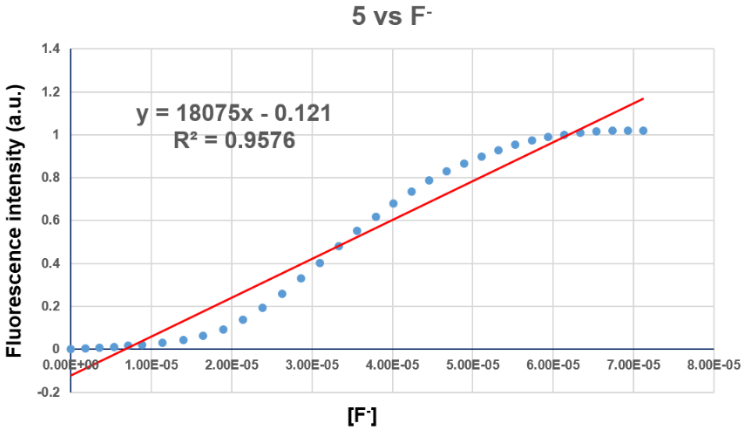

SUMMARY OUTPUT	
Regression Statistics	
Multiple R	0.978581546
R Square	0.957621843
Adjusted R Square	0.956297526
Standard Error	0.085657715
Observations	34

	Coefficients	Standard Error
Intercept	-0.12095678	0.028284975
X Variable 1 (slope)	18075.46274	672.1844258

Figure S27: Plot of absorbance of **5** (120 µM) at 396 nm against the concentration of TBAF·3H_2O in acetonitrile.

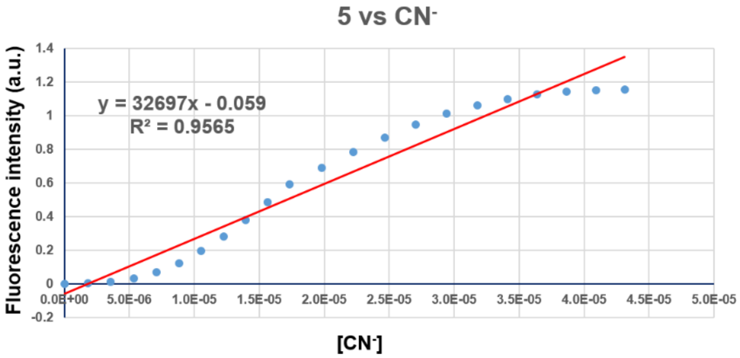

SUMMARY OUTPUT	
Regression Statistics	
Multiple R	0.97801343
R Square	0.95651026
Adjusted R Square	0.95433578
Standard Error	0.09625935
Observations	22

	Coefficients	Standard Error
Intercept	-0.0589607	0.037594935
X Variable 1 (slope)	32697.0547	1558.985987

Figure S28: Plot of absorbance of **5** (120 µM) at 395 nm against the concentration of TBACN in acetonitrile.

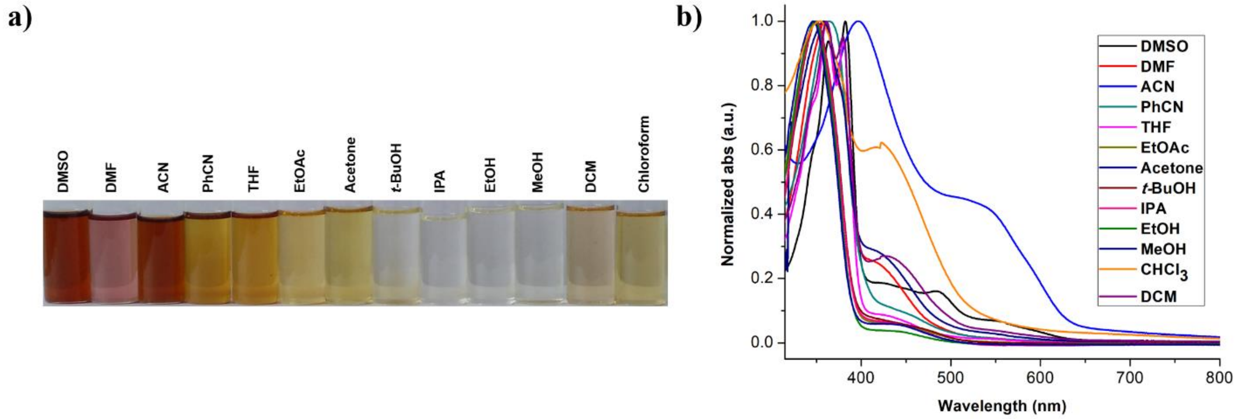

Figure S29: Visible color changes (a) and corresponding UV-vis absorption spectra (b) of **5 + F$^-$** in different solvents.

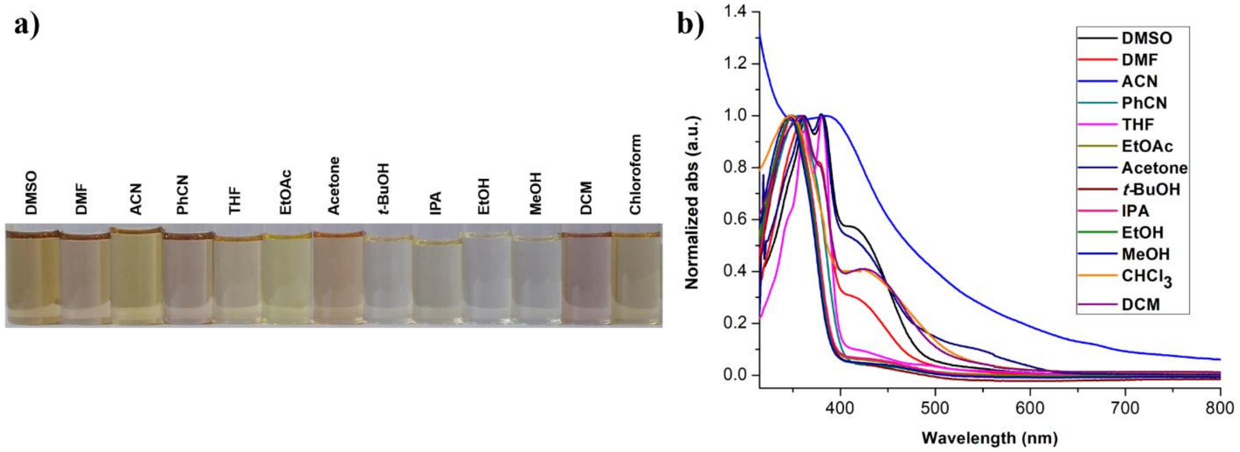

Figure S30: Visible color changes (a) and corresponding UV-vis absorption spectra (b) of **5 + CN$^-$** in different solvents.

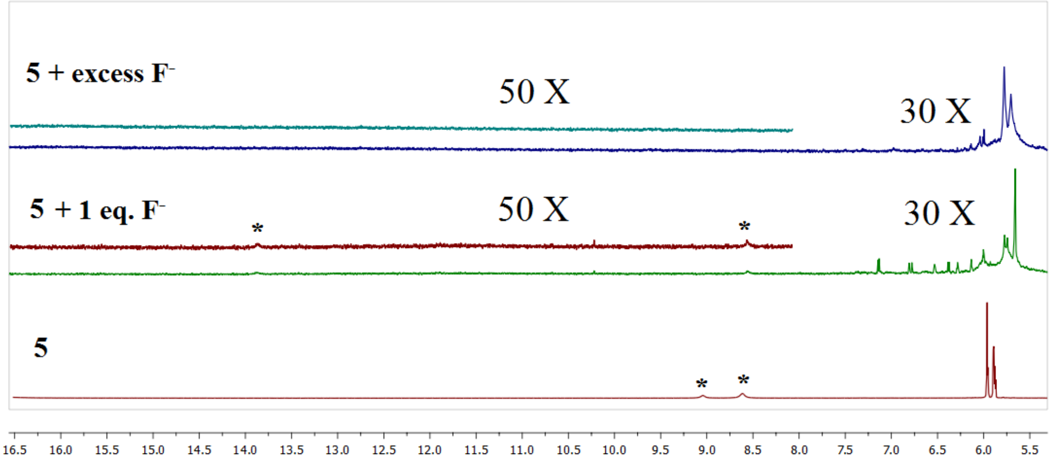

Figure S31: Partial ^{1}H NMR titration spectra of **5** (10 mM) after the addition of TBAF·$3H_2O$ in acetonitrile-d_3. '*' pyrrole NH resonance signal.

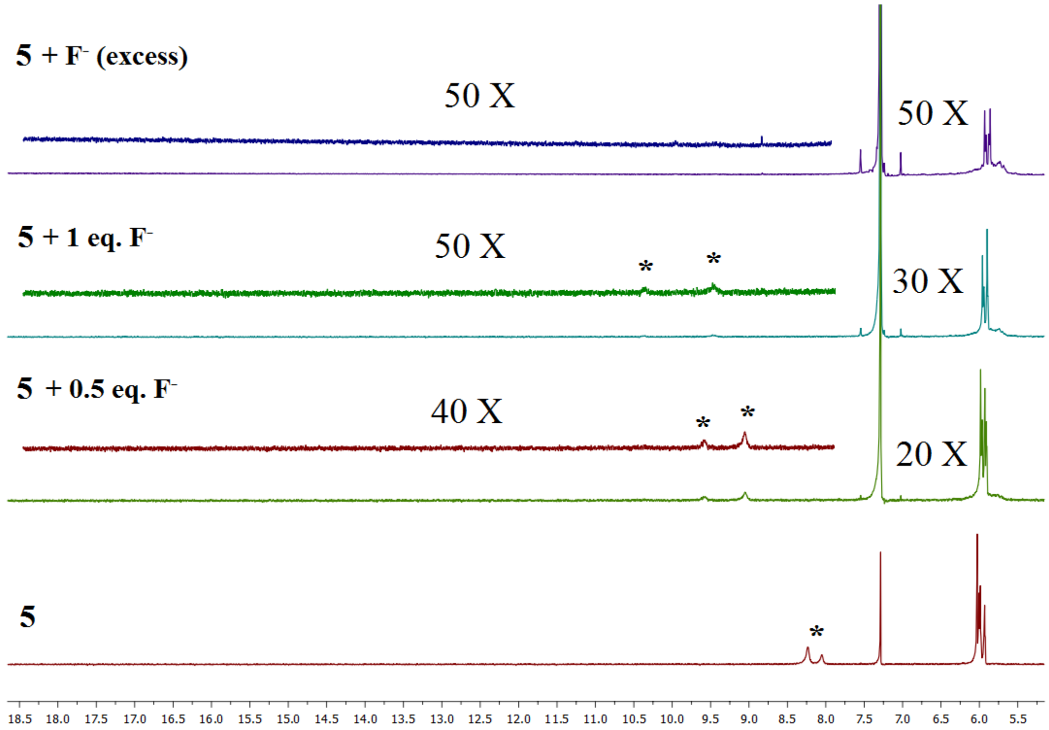

Figure S32: Partial ^{1}H NMR titration spectra of **5** (10 mM) after the addition of TBAF·$3H_2O$ in chloroform-*d*. '*' pyrrole NH resonance signal.

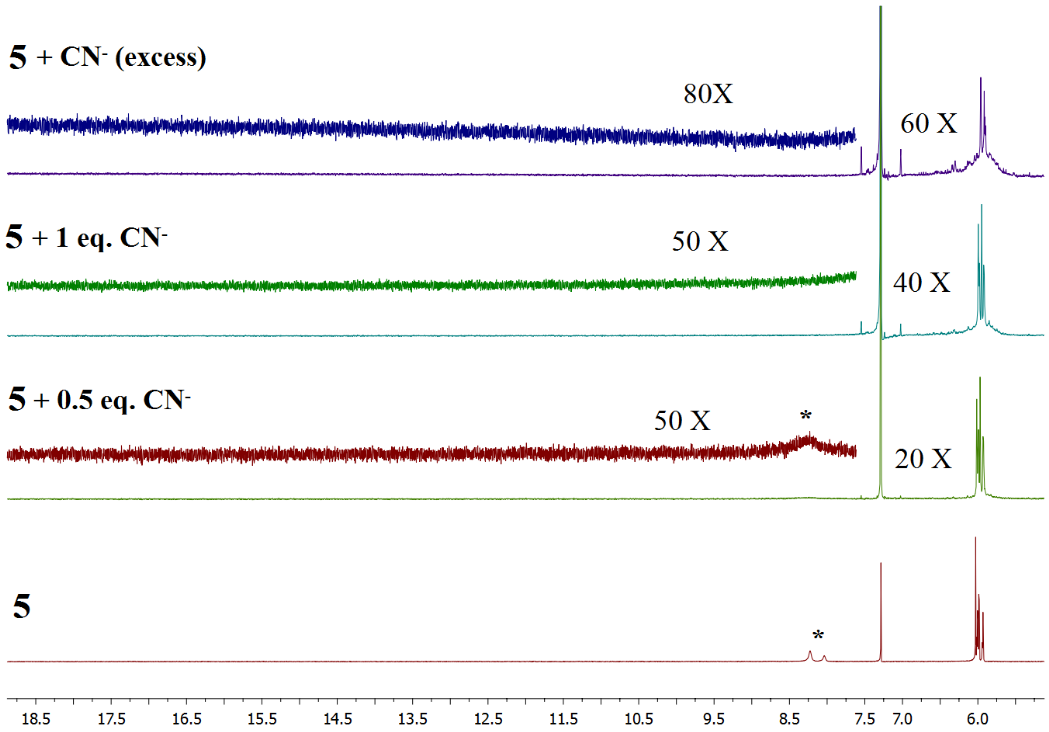

Figure S33: Partial ^{1}H NMR titration spectra of **5** (10 mM) after the addition of TBACN in chloroform-*d.* '*' pyrrole NH resonance signal.

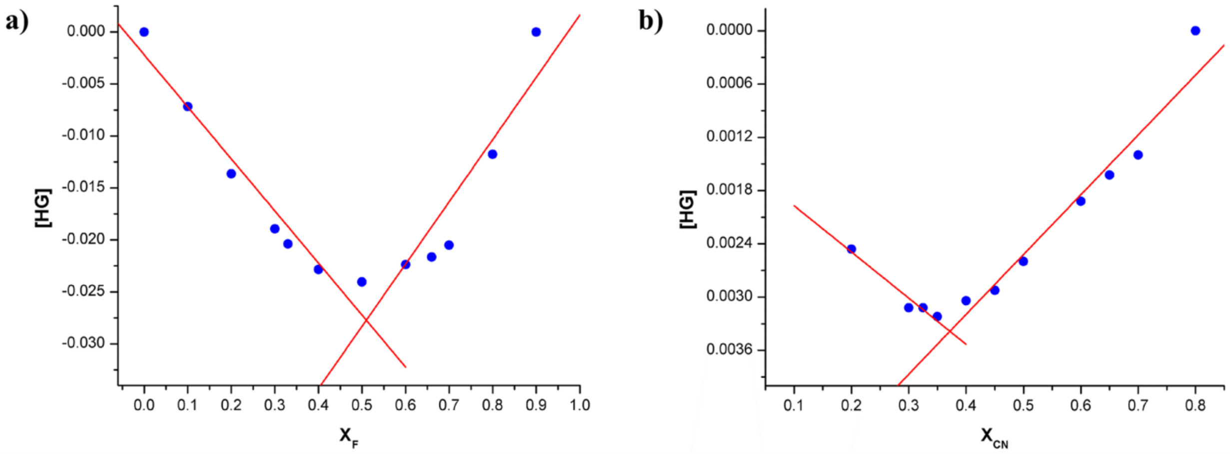

Figure S34: Job's plot analysis done by ^{1}H NMR spectral changes for **5** (10 mM) in chloroform-*d*. a) **5** vs TBAF·3H_2O and b) **5** vs TBACN.

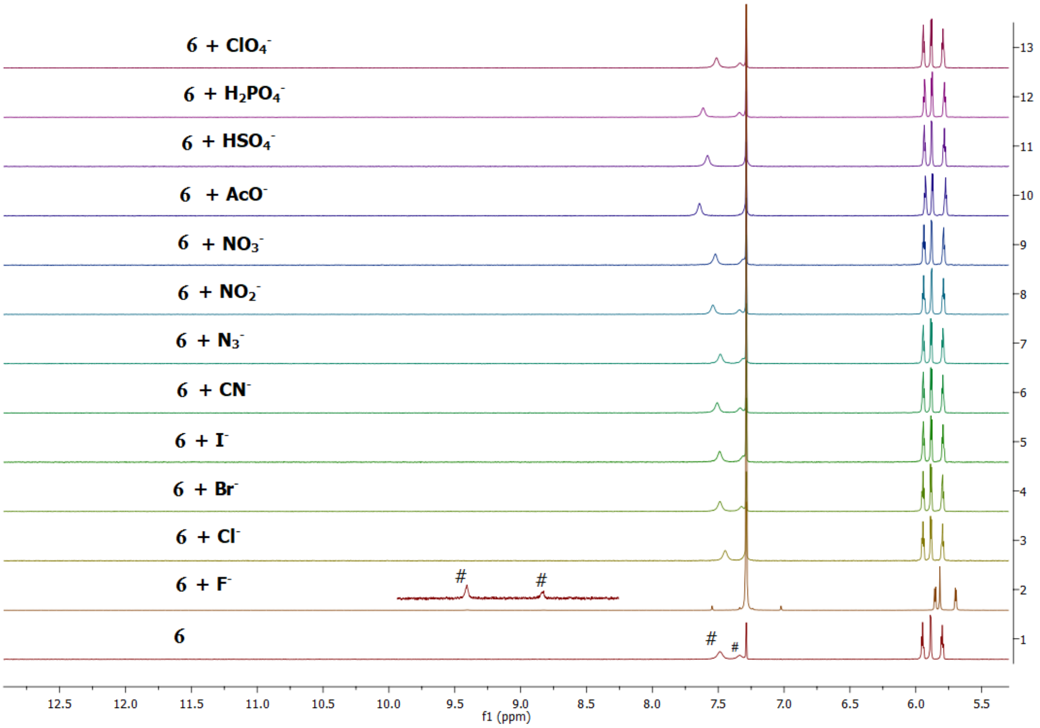

Figure S35: Partial ^{1}H NMR titration spectra of **6** (10 mM) in presence of various anions (5-15 eq.) used as their tetrabutylammonium salts in chloroform-*d*. '#' pyrrole NH resonance signal.

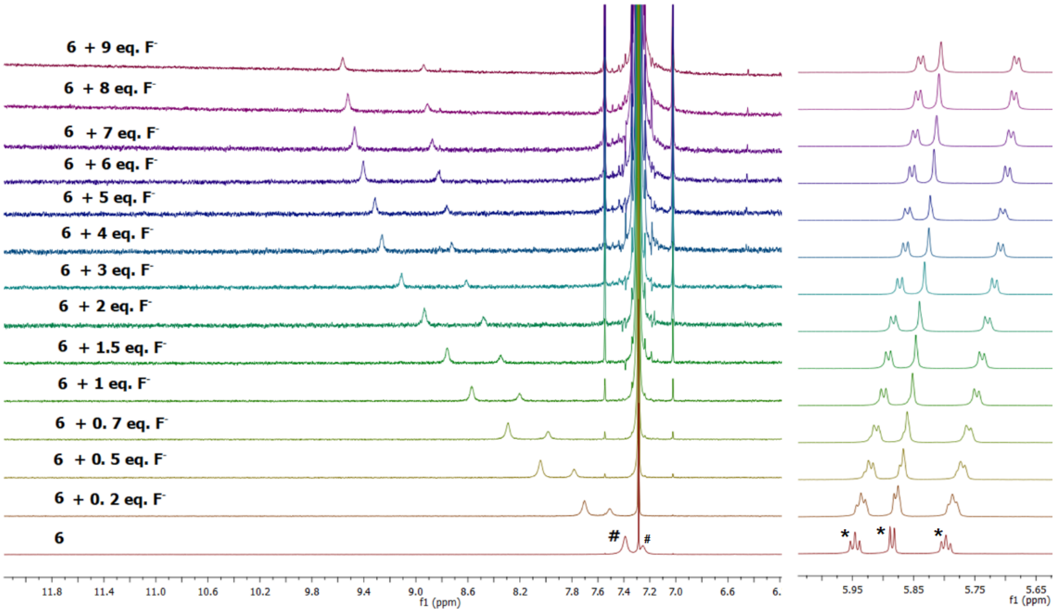

Figure S36: Partial ^{1}H NMR titration spectra of **6** (12 mM) with the gradual addition of TBAF·3H$_2$O in chloroform-*d*. '#' pyrrole NH resonance signal and '*' pyrrole *β*-CH resonance signal.

Details

Time to fit	0.2301 s
SSR	3.5030e-2
Fitted datapoints	23
Fitted params	2

Parameters

Parameter (bounds)	Optimised	Error	Initial
K (0 → ∞)	147.43 M⁻¹	± 5.7574 %	50.00 M⁻¹

Figure S37: Assessment of binding constant (K_a) by ^{1}H NMR titration study of **6** (12 mM) with the gradual addition of TBAF·3H$_2$O in chloroform-*d*.[15]

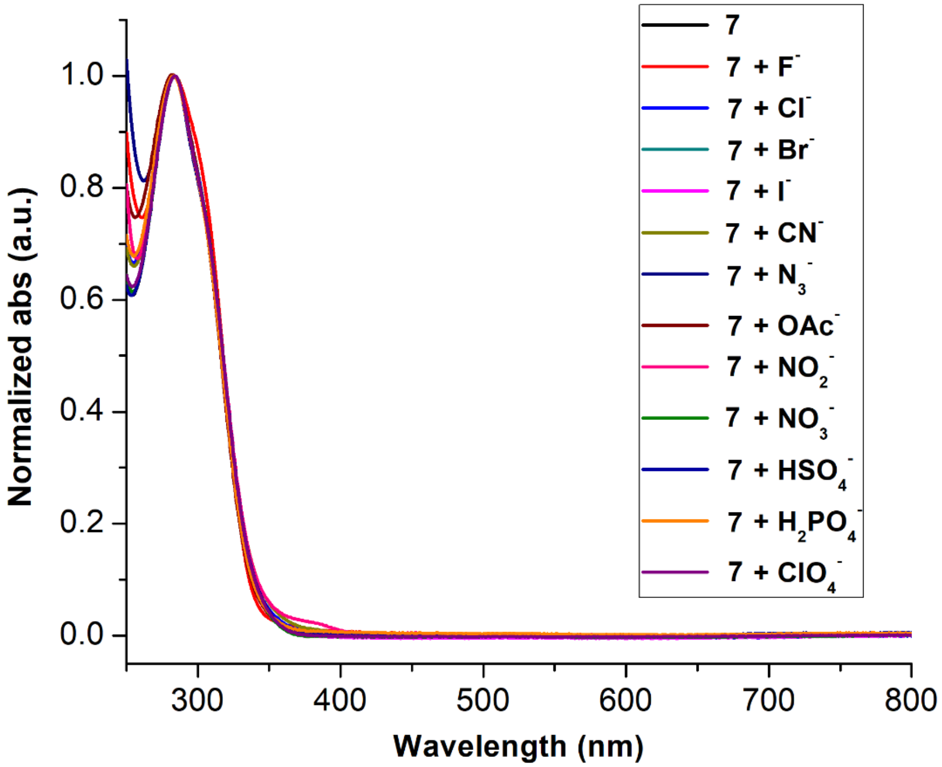

Figure S38: UV-vis spectral changes of **7** (50 µM) in presence of various anions (excess) as their tetrabutyl ammonium salts in acetonitrile.

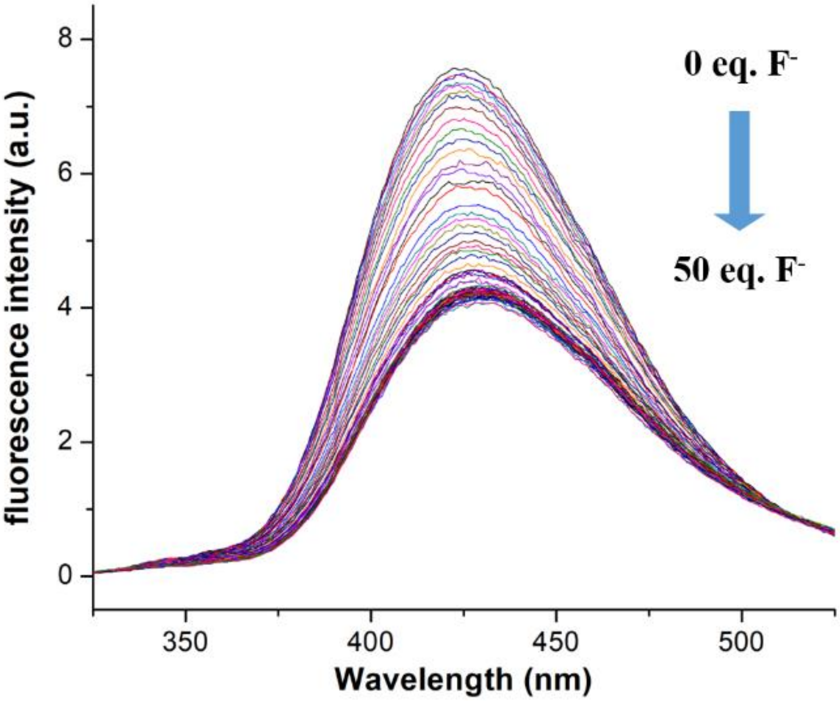

Figure S39: Fluorescence spectra of **7** (10 µM) in acetonitrile excited at 280 nm, showing induced changes of quenching upon gradual addition of TBAF·$3H_2O$.

Details

Time to fit	0.4287 s
SSR	0.0654
Fitted datapoints	61
Fitted params	2

Parameters

Parameter (bounds)	Optimised	Error	Initial
K (0 → ∞)	111379.31 M⁻¹	± 11.4589 %	1000.00 M⁻¹

Figure S40: Assessment of binding constant (K_a) by fluorometric titration study of **7** (10 µM) with the gradual addition of TBAF·$3H_2O$ in acetonitrile.[16]

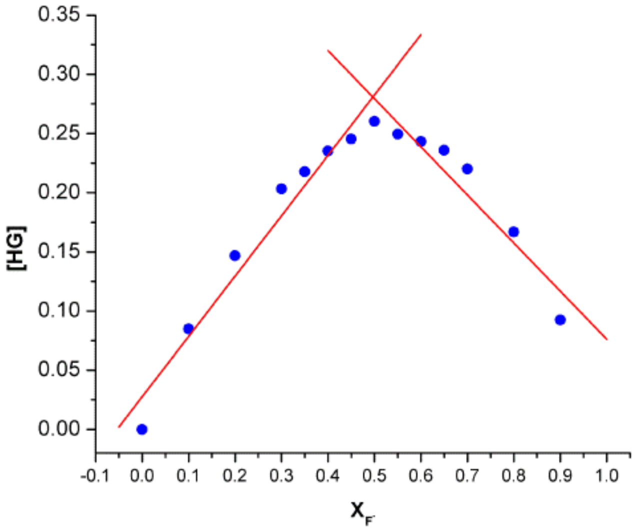

Figure S41: Job's plot analysis performed by fluorescence titration experiments of **7** (Host) (10 µM) vs TBAF·3H_2O (Guest) in acetonitrile.

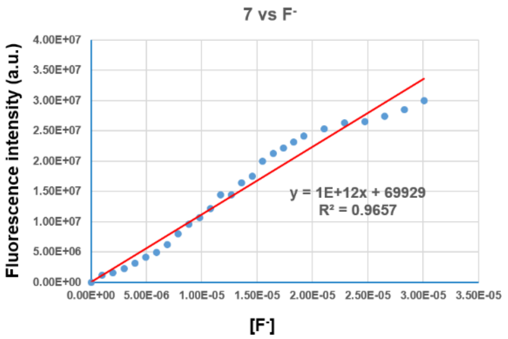

Regression Statistics	
Multiple R	0.982684712
R Square	0.965669243
Adjusted R Square	0.964296013
Standard Error	1855085.178
Observations	27

	Coefficients	Standard Error
Intercept	69928.6897	662503.7478
X Variable 1 (slope)	1.11611E+12	42088546997

Figure S42: Plot of fluorescence intensity of **7** (10 µM) at 425 nm against the concentration of TBA·3H_2O in acetonitrile.

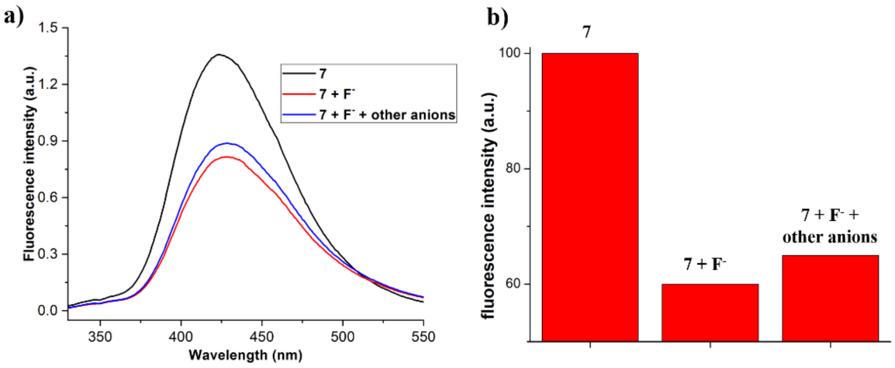

Figure S43: Competition experiment 1. a) Fluorescence spectra of **7** in acetonitrile (10 µM) excited at 280 nm showing the induced changes upon addition of excess quantities of anions as their TBA salts (other anions are Cl^-, Br^-, I^-, CN^-, AcO^-, $H_2PO_4^-$, HSO_4^-, ClO_4^-, NO_3^-, NO_2^- and N_3^-), subsequent addition of the fluoride ion; b) Corresponding bar graph of intensity at wavelength 425 nm of **7** and their anionic complexes.

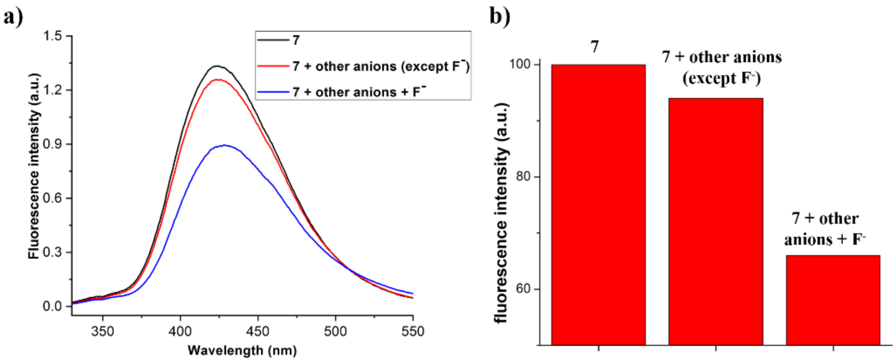

Figure S44: Competition experiment 2. a) Fluorescence spectra of **7** in acetonitrile (10 µM) excited at 280 nm showing the induced changes upon addition of the fluoride ion and subsequently excess quantities of other anions as their TBA salts (other anions are Cl^-, Br^-, I^-, CN^-, AcO^-, $H_2PO_4^-$, HSO_4^-, ClO_4^-, NO_3^-, NO_2^- and N_3^-); b) Corresponding bar graph of intensity at wavelength 425 nm of **7** and their anionic complexes.

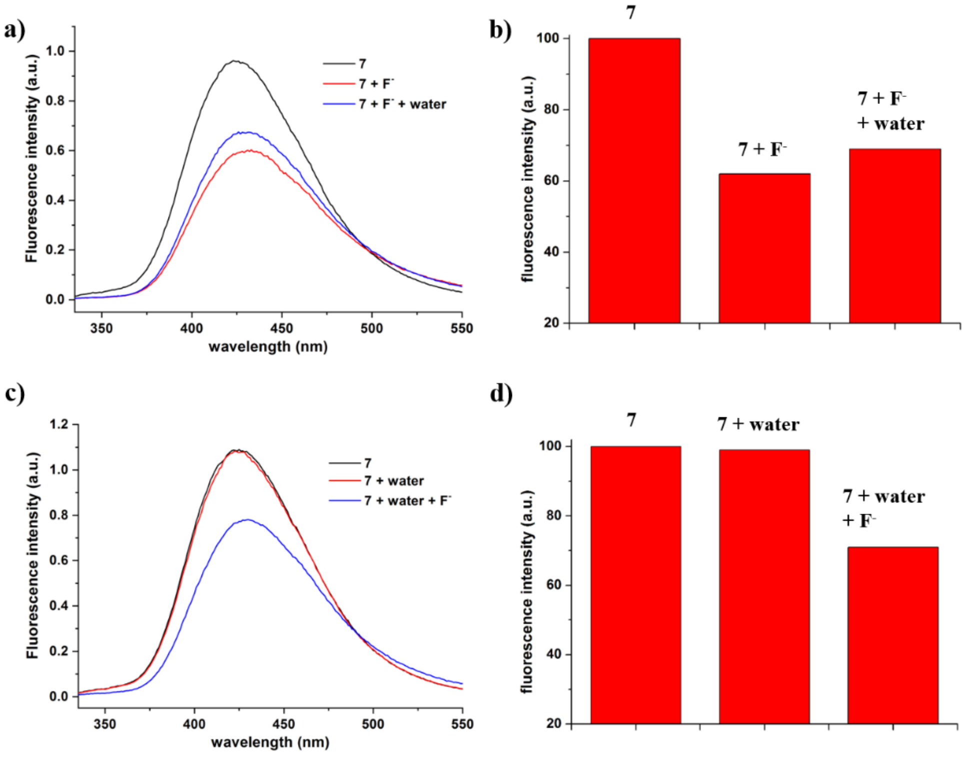

Figure S45: Effect of water (~ 0.3%) on the fluorescence spectrum of **7** (10 µM) excited at 280 nm before and after the addition of TBAF·$3H_2O$ in acetonitrile solution. (a) & (c) are fluorescence spectra of tested samples and (b) & (d) are corresponding bar graph of the intensity of tested samples at 425 nm.

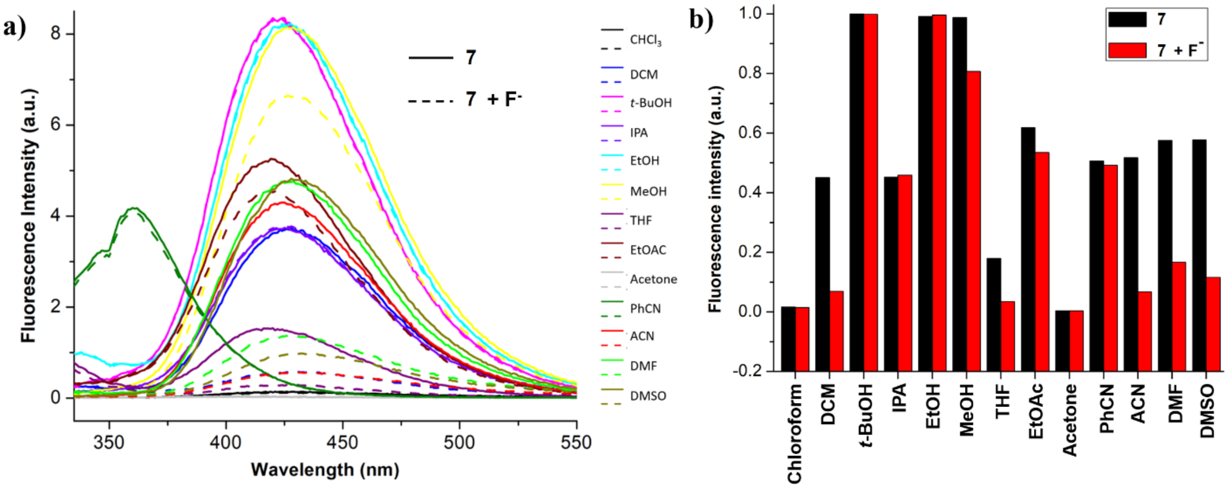

Figure S46: Effect of different solvents on the fluorescence of **7** and its fluoride complex. a) Fluorescence spectra and b) corresponding relative bar graph at emission maximum.

7) Computational study:

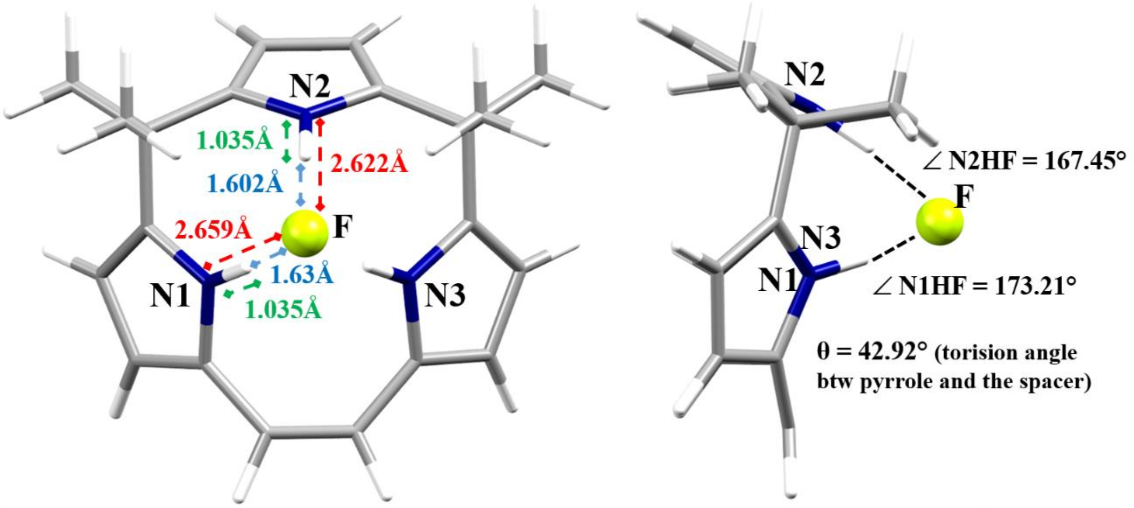

Figure S47: 5 vs F$^-$ (1:1) complex DFT optimized structure in two different views with selected bond distances and angles; color code: grey = carbon, white = hydrogen, blue = nitrogen and yellow green = fluoride ion.

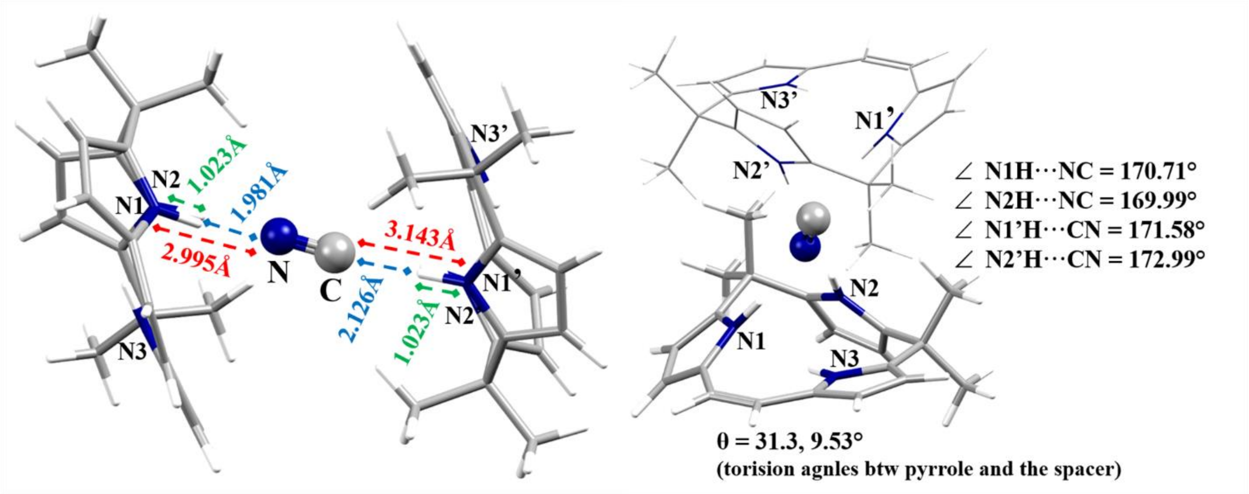

Figure S48: 5 vs CN$^-$ (2:1) complex optimized structure in two different views with selected bond distances and angles; color code: grey = carbon, white = hydrogen and blue = nitrogen.

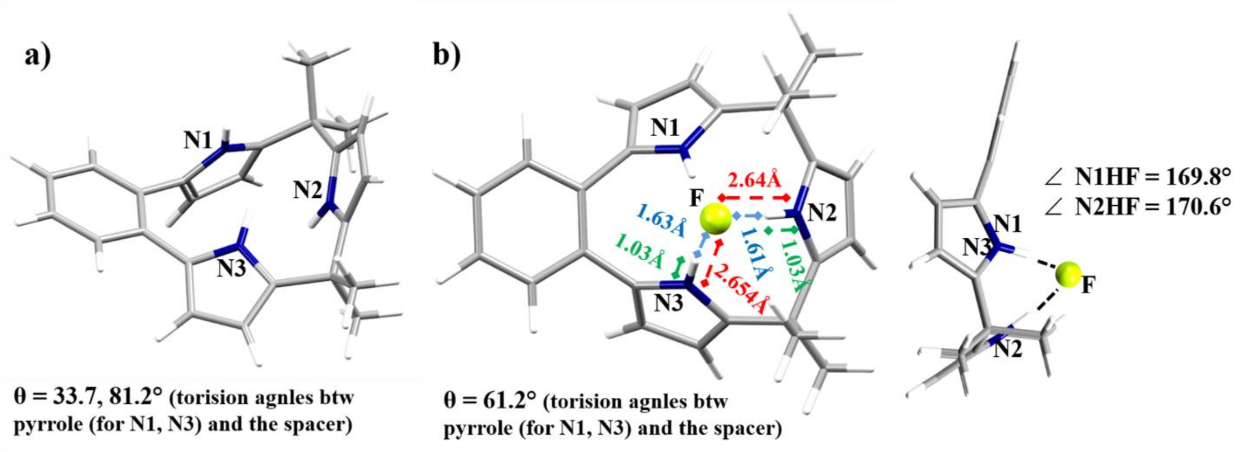

Figure S49: 7 and 7 vs F$^-$ (1:1) complex optimized structures in different views with selected bond distances and angles; color code: grey = carbon, white = hydrogen, blue = nitrogen and yellow-green = fluoride ion.

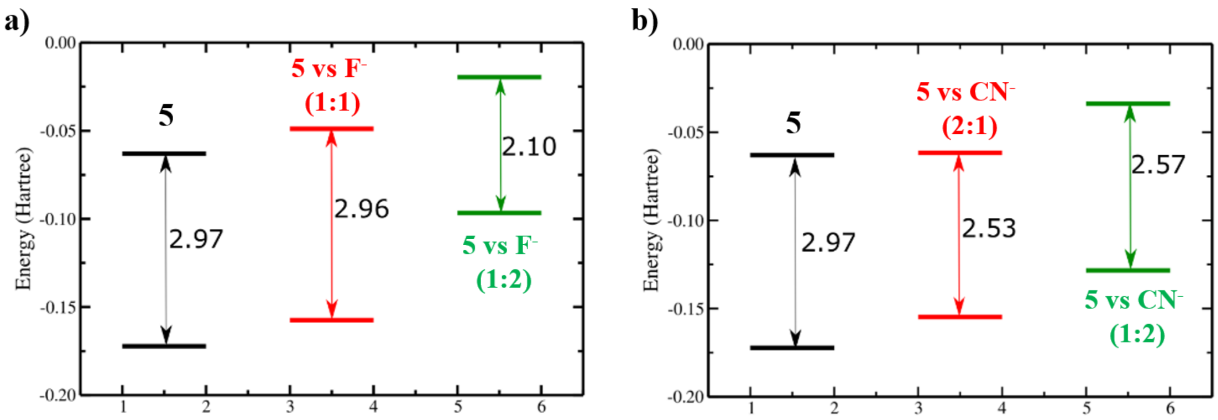

Figure S50: Representation of HOMO-LUMO gaps (eV) of host-guest complexes obtained from TD-DFT calculations in acetonitrile solvent.

Table S8: Major contributions for the electronic transitions obtained by TD-DFT data of **5** and its complexes with fluoride and cyanide ion.

S. No	**MO levels**	**Wavelength (nm)**	**Oscillator strength**	**Band Gap (eV)**
5	H → L	412.6	0.157	2.97
	H−1→ L	362.2	0.152	
	H → L+1	307.4	0.094	
	H → L+2	252.0	0.233	
$5: F^-$	H −1 → L	376.7	0.033	2.96
	H → L	360.3	0.295	
	H → L+1	284.1	0.153	
	H−1 → L+1	271.8	0.133	
$5:2F^-$	H → L	472.5	0.188	2.10
	H−1 → L	417.27	0.122	
	H → L+1	360.35	0.218	
	H−1 → L+1	277.05	0.171	
$5:CN^-$	H → L+1	416.85	0.25	2.53
	H → L+1	365.84	0.33	
	H−1 → L+2	291.20	0.23	
$5: 2CN^-$	H−1 → L+2	291.20	0.21	2.57

Table S9: Major contributions for the electronic transitions obtained from theoretical emission spectrum calculation of **7** and its complex with fluoride ion.

Sr. No	**Molecular orbital level**	**Wavelength (nm)**	**Oscillator strength (*f*)**
7	L → H	540.51	0.083
	L+1 → H	396.90	0.210
	L+1 → H−1	364.61	0.319
	L+1 → H−1	329.36	0.386
	L+1 → H−2	310.56	0.016
7: F^-	L → H	578.64	0.011
	L → H-2	402.67	0.073
	L → H−1	372.79	0.322
	L+2 → H	317.15	0.214

Table S10: Cartesian coordinates (in Å) of the DFT-optimized structure 5.

Sl. No.	Symbol	X	Y	Z	Sl. No.	Symbol	X	Y	Z
1	N	-0.1604	-1.4792	0.5139	24	C	0.8189	3.3516	-0.4725
2	N	1.423	0.985	0.1521	25	H	1.3161	4.2808	-0.7428
3	N	-1.4554	1.0832	-0.3962	26	C	3.1116	2.1969	-0.6474
4	C	1.0694	-1.8416	-0.0389	27	H	3.6895	3.0155	-1.0519
5	C	0.7935	-2.3669	-1.2925	28	C	3.5684	-2.1463	0.0113
6	H	1.5232	-2.7165	-2.0069	29	H	3.6297	-2.0817	-1.079
7	C	-0.6213	-2.2848	-1.5111	30	H	3.4636	-3.1986	0.2932
8	H	-1.1416	-2.5806	-2.4092	31	H	4.5091	-1.7724	0.4278
9	C	2.5187	0.1388	0.1361	32	C	-3.2167	1.1892	0.9679
10	C	-1.1995	-1.7144	-0.387	33	H	-4.0698	0.9198	1.5719
11	C	1.7461	2.2461	-0.3391	34	C	-2.6285	2.488	0.8784
12	C	-1.5142	2.4107	0.0409	35	H	-2.9452	3.3727	1.4118
13	C	2.3776	-1.3296	0.5601	36	C	-3.2416	-1.89	1.1049
14	C	-2.5984	-1.1762	-0.1158	37	H	-2.6394	-1.7625	2.0104
15	C	2.3728	-1.4409	2.1127	38	H	-3.3353	-2.9612	0.8993
16	H	3.3302	-1.0885	2.5098	39	H	-4.2416	-1.4901	1.3036
17	H	2.2287	-2.4822	2.4211	40	C	-3.498	-1.4128	-1.3596
18	H	1.5873	-0.83	2.5717	41	H	-4.5023	-1.0236	-1.1672
19	C	-2.4778	0.3244	0.1694	42	H	-3.5772	-2.4833	-1.5799
20	C	3.5891	0.8851	-0.3555	43	H	-3.0957	-0.9055	-2.2422
21	H	4.596	0.5264	-0.5049	44	H	0.4971	0.7119	0.4391
22	C	-0.5313	3.4376	-0.2857	45	H	-0.8561	0.7458	-1.1357
23	H	-0.9532	4.4386	-0.3462	46	H	-0.2969	-1.1469	1.4565

Table S11: Cartesian coordinates (in Å) of the DFT-optimized structure $5\cdot F^-$ (1:1).

Sl. No.	Symbol	X	Y	Z	Sl. No.	Symbol	X	Y	Z
1	N	1.5477	1.0673	0.4438	25	C	1.1422	-1.823	-0.3005
2	N	-1.5481	1.0667	0.4433	26	C	-0.7167	-2.4554	-1.4679
3	N	0.0006	-1.4933	0.4107	27	H	-1.3521	-2.8477	-2.2487
4	C	-0.6834	3.4348	0.1732	28	C	0.7177	-2.4554	-1.468
5	C	-2.5011	-1.2725	0.1404	29	H	1.3531	-2.8477	-2.2489
6	C	2.5019	-1.2716	0.1404	30	C	-3.6275	-1.9441	-0.673
7	C	3.6287	-1.9424	-0.673	31	H	-3.505	-1.7709	-1.7469
8	H	3.506	-1.7692	-1.747	32	H	-4.6032	-1.548	-0.372
9	H	3.6268	-3.0231	-0.4969	33	H	-3.6249	-3.0247	-0.4967
10	H	4.6041	-1.5457	-0.3721	34	C	2.7443	-1.5472	1.6547
11	C	-2.5008	0.2397	-0.1289	35	H	3.7248	-1.1558	1.9503
12	C	0.6819	3.435	0.1734	36	H	2.7291	-2.6264	1.8483
13	C	-3.2553	1.0317	-0.9972	37	H	1.9813	-1.0699	2.2775
14	H	-4.0705	0.6933	-1.6194	38	C	-2.7434	-1.5479	1.6548
15	C	2.5007	0.2406	-0.1286	39	H	-2.7276	-2.6271	1.8486
16	C	1.6421	2.3564	-0.0622	40	H	-3.7242	-1.157	1.9503
17	C	2.7339	2.3596	-0.9415	41	H	-1.9806	-1.07	2.2774
18	H	3.0691	3.2079	-1.5221	42	H	0.0014	-0.9392	1.2852
19	C	-1.1411	-1.823	-0.3003	43	H	0.951	0.795	1.2428
20	C	3.2545	1.033	-0.9972	44	H	-0.9509	0.7942	1.242
21	H	4.0696	0.6948	-1.6198	45	H	-1.1436	4.4215	0.23
22	C	-2.7351	2.3586	-0.9416	46	H	1.1416	4.422	0.2304
23	H	-3.0709	3.2068	-1.522	47	F	-0.0008	0.1918	2.42
24	C	-1.6431	2.3558	-0.0625					

Table S12: Cartesian coordinates (in Å) of the DFT-optimized structure 5·F$^-$ (1:2).

Sl. No.	Symbol	X	Y	Z	Sl. No.	Symbol	X	Y	Z
1	N	-0.0093	-1.4774	0.3816	25	H	1.1383	4.3457	0.0147
2	N	1.3021	0.9709	-0.0641	26	C	3.0319	2.3844	0.2081
3	N	-1.3458	1.0427	0.1635	27	H	3.6043	3.299	0.2922
4	C	0.944	-1.7282	-0.5508	28	C	3.2659	-1.6016	-1.52
5	C	0.344	-2.1872	-1.7569	29	H	2.9266	-1.0716	-2.4156
6	H	0.8536	-2.4802	-2.6651	30	H	3.2359	-2.6777	-1.7247
7	C	-1.0299	-2.1476	-1.5446	31	H	4.306	-1.3211	-1.327
8	H	-1.8052	-2.4158	-2.2504	32	C	-3.4739	1.0726	-0.7057
9	C	2.4056	0.2182	-0.055	33	H	-4.4517	0.7121	-0.9952
10	C	-1.2185	-1.6979	-0.2	34	C	-2.989	2.3384	-0.82
11	C	1.6064	2.3164	0.0829	35	H	-3.4871	3.2091	-1.229
12	C	-1.6158	2.2982	-0.3047	36	C	-2.4585	-1.2345	1.9797
13	C	2.3732	-1.2856	-0.2993	37	H	-1.5847	-0.7365	2.4012
14	C	-2.4813	-1.16	0.439	38	H	-2.4418	-2.2847	2.2942
15	C	2.9576	-1.9939	0.9643	39	H	-3.3617	-0.7669	2.3897
16	H	3.9918	-1.6751	1.1357	40	C	-3.7399	-1.8665	-0.0925
17	H	2.9543	-3.0764	0.8042	41	H	-4.6425	-1.4193	0.3394
18	H	2.3629	-1.7519	1.8468	42	H	-3.7189	-2.9235	0.1896
19	C	-2.4267	0.29	-0.0322	43	H	-3.821	-1.8073	-1.1829
20	C	3.5208	1.0942	0.1405	44	H	0.2484	-1.0831	1.3652
21	H	4.5567	0.7878	0.185	45	H	0.2689	0.2978	-0.8878
22	C	-0.7035	3.3547	-0.3011	46	F	-0.3836	-0.1273	-1.408
23	H	-1.1182	4.3271	-0.5576	47	F	0.3044	0.7065	2.0605
24	C	0.6853	3.3574	-0.0325	48	H	-0.3428	0.8383	1.3165

Table S13: Cartesian coordinates (in Å) of the DFT-optimized structure 5·CN$^-$ (2:1).

Sl. No.	Symbol	X	Y	Z	Sl. No.	Symbol	X	Y	Z
1	N	-3.1602	1.3125	1.188	48	N	3.1811	-1.3299	-1.1621
2	N	-3.1751	-1.639	1.2582	49	N	3.3272	0.3163	1.2777
3	N	-3.3071	-0.2966	-1.2818	50	C	3.046	-0.5899	-3.5797
4	C	-2.6446	-0.7717	3.574	51	C	3.8702	-2.1637	1.1569
5	C	-3.2969	-2.8186	-1.0153	52	C	3.2983	2.8354	0.9748
6	C	-3.8323	2.1852	-1.1229	53	C	4.2881	4.0187	1.1401
7	C	-4.8826	3.1644	-1.693	54	H	5.1913	3.8618	0.5419
8	H	-5.8943	2.9089	-1.3641	55	H	4.5805	4.1322	2.1902
9	H	-4.8588	3.1416	-2.7872	56	H	3.8157	4.9498	0.8119
10	H	-4.6638	4.186	-1.3657	57	C	3.9354	-2.2009	-0.3758
11	C	-2.8886	-2.7333	0.4631	58	C	2.6239	0.7092	-3.5753
12	C	-3.0505	0.5326	3.5944	59	C	4.7852	-2.8855	-1.239
13	C	-2.1526	-3.6181	1.2538	60	H	5.5264	-3.6145	-0.9491
14	H	-1.7674	-4.577	0.9393	61	C	2.8747	2.7216	-0.497
15	C	-3.9034	2.2006	0.4102	62	C	2.5804	1.7182	-2.536
16	C	-3.5439	1.3965	2.5305	63	C	1.9376	2.9638	-2.5615
17	C	-4.521	2.392	2.5996	64	H	1.3833	3.3609	-3.4003
18	H	-5.0465	2.6896	3.4961	65	C	4.1951	-0.7286	1.5774
19	C	-3.9557	-1.5181	-1.4495	66	C	2.1176	3.5836	-1.2928
20	C	-4.7538	2.8789	1.2782	67	H	1.7221	4.5415	-0.9887
21	H	-5.4883	3.6173	0.9947	68	C	4.54	-2.4206	-2.566
22	C	-1.9798	-3.0209	2.5342	69	H	5.0615	-2.7284	-3.4614
23	H	-1.4417	-3.4389	3.3731	70	C	3.5558	-1.4318	-2.5062
24	C	-2.605	-1.7663	2.5208	71	C	3.9669	1.5453	1.4258
25	C	-4.167	0.759	-1.5658	72	C	5.3902	-0.1477	1.9869
26	C	-5.2337	-1.2311	-1.9125	73	H	6.2856	-0.6757	2.2786
27	H	-6.002	-1.9533	-2.145	74	C	5.2474	1.2744	1.8911
28	C	-5.3658	0.1934	-1.9865	75	H	6.0111	2.0054	2.1107
29	H	-6.2568	0.7321	-2.2719	76	C	4.9294	-3.1268	1.7375
30	C	-4.2886	-3.9954	-1.2123	77	H	5.9375	-2.8701	1.3991
31	H	-5.1979	-3.8463	-0.6209	78	H	4.7155	-4.1548	1.4281
32	H	-3.8229	-4.9338	-0.8956	79	H	4.9114	-3.0863	2.8311
33	H	-4.5701	-4.089	-2.2675	80	C	2.0334	3.1202	1.8415
34	C	-2.43	2.6314	-1.6289	81	H	1.5569	4.0553	1.5278
35	H	-2.2302	3.6577	-1.3001	82	H	2.3162	3.2113	2.8963
36	H	-2.4052	2.6081	-2.7247	83	H	1.2984	2.3152	1.7438
37	H	-1.6274	1.992	-1.2519	84	C	2.4729	-2.6124	1.6737
38	C	-2.024	-3.09	-1.8744	85	H	2.4495	-2.5702	2.7688
39	H	-2.2972	-3.1657	-2.933	86	H	2.279	-3.6452	1.3622
40	H	-1.549	-4.029	-1.5701	87	H	1.6647	-1.9848	1.2877
41	H	-1.2917	-2.2849	-1.7584	88	H	2.3638	0.2035	0.9475

42	H	-2.3461	-0.1955	-0.9454	89	H	3.683	0.8155	-0.9536
43	H	-2.3094	0.8437	0.8678	90	H	2.3298	-0.8612	-0.843
44	H	-3.6711	-0.8213	0.9395	91	H	3.0503	-1.079	-4.5521
45	H	-2.2888	-1.1651	4.5246	92	H	2.2554	1.0842	-4.5285
46	H	-3.0561	1.0068	4.5742	93	C	0.5078	-0.0967	0.0541
47	N	3.1673	1.6187	-1.2783	94	N	-0.6567	0.1198	-0.0198

Table S14: Cartesian coordinates (in Å) of the DFT-optimized structure 5·CN^- (1:1).

Sl. No.	Symbol	X	Y	Z	Sl. No.	Symbol	X	Y	Z
1	N	1.5249	1.0509	0.2842	25	C	1.1293	-1.8121	-0.3759
2	N	-1.5252	1.0498	0.2841	26	C	-0.7098	-2.4435	-1.5318
3	N	0.0003	-1.4837	0.3245	27	H	-1.3499	-2.8278	-2.3138
4	C	-0.6794	3.3971	0.004	28	C	0.7101	-2.4431	-1.5322
5	C	-2.4849	-1.2679	0.0395	29	H	1.35	-2.827	-2.3144
6	C	2.4854	-1.2665	0.0381	30	C	-3.5784	-1.9361	-0.7965
7	C	3.5787	-1.9338	-0.7989	31	H	-3.4298	-1.7543	-1.8643
8	H	3.429	-1.7521	-1.8666	32	H	-4.5615	-1.5451	-0.5167
9	H	3.5745	-3.0145	-0.6283	33	H	-3.5734	-3.0167	-0.6258
10	H	4.5617	-1.5422	-0.5198	34	C	2.7743	-1.5436	1.5263
11	C	-2.4809	0.2289	-0.2452	35	H	3.7631	-1.1525	1.7891
12	C	0.6767	3.3974	0.0037	36	H	2.7634	-2.6226	1.7163
13	C	-3.2479	1.0034	-1.1015	37	H	2.0447	-1.0731	2.1906
14	H	-4.0673	0.651	-1.7125	38	C	-2.7723	-1.5447	1.528
15	C	2.4802	0.2303	-0.2465	39	H	-2.7605	-2.6236	1.7185
16	C	1.6335	2.3217	-0.2148	40	H	-3.7612	-1.1542	1.7915
17	C	2.73	2.322	-1.0687	41	H	-2.0424	-1.0734	2.1915
18	H	3.0608	3.1646	-1.6613	42	H	0	-1.0049	1.2286
19	C	-1.1288	-1.8128	-0.3754	43	H	0.9689	0.8221	1.1127
20	C	3.2449	1.0049	-1.1047	44	H	-0.9677	0.8207	1.1115
21	H	4.0633	0.6527	-1.7171	45	H	-1.1404	4.3827	0.0542
22	C	-2.7339	2.3209	-1.0655	46	H	1.1371	4.3834	0.0537
23	H	-3.0666	3.1637	-1.6569	47	N	-0.0004	0.2862	2.6383
24	C	-1.6358	2.3208	-0.2137	48	C	0.0106	0.2269	3.8189

Table S15: Cartesian coordinates (in Å) of the DFT-optimized structure 5·CN$^-$ (1:2).

Sl. No.	Symbol	X	Y	Z	Sl. No.	Symbol	X	Y	Z
1	N	-0.0662	-1.3794	0.5334	26	C	2.7487	2.1455	1.1437
2	N	1.499	0.9577	-0.3386	27	H	3.0883	2.9608	1.779
3	N	-1.4903	1.1797	0.3585	28	C	3.1162	-1.5778	-1.4484
4	C	0.9386	-1.8813	-0.2474	29	H	2.6193	-0.9783	-2.2162
5	C	0.3564	-2.75	-1.1649	30	H	3.1297	-2.6343	-1.7582
6	H	0.8732	-3.3008	-1.9421	31	H	4.1568	-1.2391	-1.3488
7	C	-1.0525	-2.7047	-0.958	32	C	-3.2858	1.0021	-0.95
8	H	-1.8057	-3.207	-1.5549	33	H	-4.1574	0.6025	-1.4559
9	C	2.3775	0.1088	0.2581	34	C	-2.6772	2.2648	-1.1821
10	C	-1.2872	-1.814	0.0849	35	H	-2.9843	3.0144	-1.9049
11	C	1.6789	2.1945	0.2284	36	C	-2.716	-1.1216	2.0709
12	C	-1.5342	2.3352	-0.3795	37	H	-1.8577	-0.6047	2.5209
13	C	2.3768	-1.3818	-0.1004	38	H	-2.755	-2.1596	2.4349
14	C	-2.5723	-1.1035	0.5261	39	H	-3.6467	-0.615	2.3684
15	C	3.1024	-2.1925	1	40	C	-3.7874	-1.817	-0.0921
16	H	4.1495	-1.8746	1.104	41	H	-4.7167	-1.3149	0.206
17	H	3.0916	-3.2624	0.7512	42	H	-3.8296	-2.8582	0.2516
18	H	2.6074	-2.0569	1.9676	43	H	-3.7359	-1.8187	-1.1861
19	C	-2.5157	0.3416	0.0067	44	H	0.042	-0.6604	1.3212
20	C	3.1816	0.8038	1.1791	45	H	-0.8301	0.9708	1.1685
21	H	3.948	0.3865	1.8255	46	H	1.1678	0.7467	-1.8233
22	C	-0.5286	3.3925	-0.3056	47	C	1.2215	0.6005	-2.8031
23	H	-0.9247	4.3876	-0.5276	48	N	1.2843	0.415	-3.9329
24	C	0.8019	3.3305	-0.0121	49	C	-0.168	0.353	2.3752
25	H	1.2927	4.304	0.0987	50	N	0.3969	-0.0892	3.2696

Table S16: Cartesian coordinates (in Å) of the DFT-optimized structure 7.

Sl. No.	Symbol	X	Y	Z	Sl. No.	Symbol	X	Y	Z
1	N	-0.3065	-1.7771	-0.2746	27	H	-3.632	-2.8096	-0.1262
2	N	-0.4154	1.3162	-0.0456	28	C	-4.0708	0.9945	-0.5982
3	N	2.1543	0.0329	0.2599	29	H	-4.1859	2.0617	-0.753
4	C	-2.6668	-0.8992	0.0053	30	C	2.1774	-3.4284	-1.2972
5	C	-1.4281	-1.5325	0.5245	31	H	1.8863	-4.4343	-0.9789
6	C	0.304	2.4562	0.2732	32	H	3.1895	-3.4767	-1.7137
7	C	0.723	-2.3427	0.4817	33	H	1.5005	-3.1111	-2.0978
8	C	-1.78	1.5151	0.1306	34	C	2.4404	2.8117	1.5715
9	C	-2.8162	0.5122	-0.1586	35	H	2.1987	2.0087	2.2765
10	C	2.3791	1.2364	-0.4023	36	H	2.0401	3.7445	1.9826
11	C	1.8341	2.5372	0.1621	37	H	3.5307	2.8955	1.504
12	C	2.1344	-2.4588	-0.0889	38	C	-5.1437	0.1429	-0.853
13	C	2.522	-1.0496	-0.532	39	H	-6.0901	0.5558	-1.1884
14	C	-0.627	3.4114	0.6731	40	C	-4.9933	-1.2384	-0.6903
15	H	-0.4039	4.4158	1.0007	41	H	-5.8195	-1.9128	-0.8904
16	C	-1.9224	2.8299	0.5795	42	C	3.1036	-2.983	1.0031
17	H	-2.8551	3.305	0.8442	43	H	3.1397	-2.3064	1.8629
18	C	3.043	-0.5211	-1.7033	44	H	4.1144	-3.0597	0.5909
19	H	3.422	-1.0849	-2.542	45	H	2.7929	-3.9736	1.3542
20	C	2.9547	0.9082	-1.621	46	C	2.2175	3.7082	-0.7785
21	H	3.2502	1.6055	-2.3895	47	H	3.3069	3.7887	-0.8658
22	C	-1.1075	-1.9713	1.7976	48	H	1.8316	4.6518	-0.3813
23	H	-1.7561	-1.9111	2.6582	49	H	1.7936	3.5613	-1.7763
24	C	0.2363	-2.468	1.7739	50	H	1.6977	-0.0632	1.1547
25	H	0.7844	-2.8537	2.6196	51	H	-0.2742	-1.6372	-1.2733
26	C	-3.7619	-1.7413	-0.2673	52	H	0.0009	0.457	-0.364

Table S17: Cartesian coordinates (in Å) of the DFT-optimized structure 7·F$^-$ (1:1).

Sl. No.	Symbol	X	Y	Z	Sl. No.	Symbol	X	Y	Z
1	N	-0.4238	1.563	0.3328	28	C	-5.2123	0.6998	0.3626
2	N	-0.424	-1.563	0.3328	29	H	-6.1328	1.2523	0.5237
3	N	2.139	0.0002	0.5446	30	C	3.4105	-0.7175	-1.1399
4	C	-2.7873	-0.7162	-0.0553	31	H	3.928	-1.3529	-1.8442
5	C	1.9484	-2.492	0.2329	32	C	3.411	0.7174	-1.1397
6	C	1.9489	2.492	0.2332	33	H	3.9288	1.3527	-1.8439
7	C	2.6952	3.6203	-0.5083	34	C	-4.0129	-1.3844	0.1586
8	H	2.6833	3.4645	-1.5917	35	H	-4.0079	-2.4697	0.157
9	H	3.7392	3.6588	-0.18	36	C	2.6948	-3.62	-0.5092
10	H	2.2299	4.5887	-0.2965	37	H	2.6826	-3.4639	-1.5926
11	C	0.4885	-2.4359	-0.2413	38	H	2.2296	-4.5885	-0.2976
12	C	-2.7871	0.7166	-0.0555	39	H	3.7388	-3.6585	-0.1812
13	C	-0.151	-3.0349	-1.3261	40	C	2.01	2.7694	1.7641
14	H	0.2846	-3.7561	-2.0016	41	H	1.5513	3.74	1.9869
15	C	0.489	2.4358	-0.2411	42	H	3.054	2.7948	2.0983
16	C	-1.6143	1.564	-0.3781	43	H	1.4822	1.9991	2.3351
17	C	-1.4713	2.4976	-1.4064	44	C	2.0101	-2.7699	1.7636
18	H	-2.2203	2.7327	-2.1494	45	H	3.0541	-2.7954	2.0974
19	C	2.5862	-1.1405	-0.0987	46	H	1.5515	-3.7407	1.9863
20	C	-0.1502	3.0348	-1.3261	47	H	1.4824	-1.9998	2.3349
21	H	0.2857	3.7559	-2.0015	48	C	-5.2124	-0.6987	0.3629
22	C	-4.0126	1.3852	0.1582	49	H	-6.133	-1.2509	0.5242
23	H	-4.0073	2.4705	0.1562	50	H	1.468	0.0009	1.3333
24	C	-1.4721	-2.4976	-1.4061	51	H	-0.25	1.003	1.1863
25	H	-2.2213	-2.7327	-2.149	52	H	-0.2495	-1.0037	1.1869
26	C	-1.6147	-1.5639	-0.3777	53	F	0.2356	-0.0016	2.376
27	C	2.5867	1.1406	-0.0986					

8) References:

1. SAINT, version 6.45 /8/6/03 and version 8.34A, Bruker AXS, **2003, 2014**.
2. G. M. Sheldrick, SADABS 2014/5, *Program for Empirical Absorption Correction of Area Detector Data*, University of Göttingen, Germany, **1997, 2014**.
3. (a) G. M. Sheldrick, *SHELXS-97* and *SHELXL-97, Programs for the Solution and Refinement of Crystal Structures*, University of Göttingen, Germany, **1997**; (b) SHELXL -Version 2014/7; *Program for the Solution and Refinement of Crystal Structures*, University of Göttingen, Germany, 1993-2014; G. M. Sheldrick, *Acta Cryst.* **2008**, *A64*, 112.
4. (a) A. L. Spek, *PLATON, A Multipurpose Crystallographic Tool*, Utrecht University, Utrecht, The Netherlands, **2002**; (b) A. L. Spek, *J. Appl. Cryst.* **2003**, *36*, 7.
5. Y. Zhao, D. G. Truhlar, Hybrid Meta Density Functional Theory Methods for Thermochemistry, Thermochemical Kinetics, and Noncovalent Interactions: The MPW1B95 and MPWB1K Models and Comparative Assessments for Hydrogen Bonding and van der Waals Interactions, *J. Phys. Chem. A* **2004**, *108*, 6908.
6. C. Adamo, V. Barone, Exchange functionals with improved long-range behavior and adiabatic connection methods without adjustable parameters: The *m*PWmPW and *m*PW1PWmPW1PW models, *J. Chem. Phys*. **1998**, *108*, 664.
7. R. Ditchfield, W. J. Hehre, J. A. Pople, *J. Chem. Phys*. **1971**, *54*, 724.
8. Gaussian 09, Revision E.01, M. J. Frisch, G. W. Trucks, H. B. Schlegel, G. E. Scuseria, M. A. Robb, J. R. Cheeseman, G. Scalmani, V. Barone, B. Mennucci, G. A. Petersson, H. Nakatsuji, M. Caricato, X. Li, H. P. Hratchian, A. F. Izmaylov, J. Bloino, G. Zheng, J. L. Sonnenberg, M. Hada, M. Ehara, K. Toyota, R. Fukuda, J. Hasegawa, M. Ishida, T. Nakajima, Y. Honda, O. Kitao, H. Nakai, T. Vreven, J. A. Montgomery, Jr., J. E. Peralta, F. Ogliaro, M. Bearpark, J. J. Heyd, E. Brothers, K. N. Kudin, V. N. Staroverov, R. Kobayashi, J. Normand, K. Raghavachari, A. Rendell, J. C. Burant, S. S. Iyengar, J. Tomasi, M. Cossi, N. Rega, J. M. Millam, M. Klene, J. E. Knox, J. B. Cross, V. Bakken, C. Adamo, J. Jaramillo, R. Gomperts, R. E. Stratmann, O. Yazyev, A. J. Austin, R. Cammi, C. Pomelli, J. W. Ochterski, R. L. Martin, K. Morokuma, V. G. Zakrzewski, G. A. Voth, P. Salvador, J. J. Dannenberg, S. Dapprich, A. D. Daniels, Ö. Farkas, J. B. Foresman, J. V. Ortiz, J. Cioslowski and D. J. Fox, *Gaussian, Inc.*, Wallingford CT, **2009**.
9. A. V. Marenich, C. J. Cramer, D. G. Truhlar, *J. Phys. Chem. B.* **2009**, *113*, 6378.
10. (a) C. Bucher, R. S. Zimmerman, V. Lynch, J. L. Sessler, *J. Am. Chem. Soc.* **2001**, *123*, 9716; (b) C. Bucher, R. S. Zimmerman, V. Lynch, V. Král, J. L. Sessler, *J. Am. Chem. Soc*. **2001**, *123*, 2099.
11. (a) S. P. Mahanta, B. S. Kumar, S. Baskaran, C. Sivasankar, P. K. Panda, *Org. Lett.* **2012**, *14*, 548; (b) B. Chandra, S. P. Mahanta, N. N. Pati, S. Baskaran, R. K. Kanaparthi, C. Sivasankar, P. K. Panda, *Org. Lett.* **2013**, *15*, 306.
12. http://app.supramolecular.org/bindfit/view/e0cc5ed5-df52-455b-9053-16a209e5af08
13. http://app.supramolecular.org/bindfit/view/1588cbbb-7dd0-4e16-9deb-554305b63eb2
14. (a) http://www.ich.org/products/guidelines/quality/article/quality-guidelines.html; (b) A. Shrivastava, V. B. Gupta, *Chron Young Sci.* **2011**, *2*, 21.
15. http://app.supramolecular.org/bindfit/view/5859ee46-fcff-463f-b736-49a0fb14fef0
16. http://app.supramolecular.org/bindfit/view/99df3439-6388-4a0d-9480-5cad5f07c699